Supporting Information

Tetraphenylethylene Tricycle-based Sequential Light-Harvesting System through Efficient Förster Resonance Energy Transfer for Visible Light Photocatalysis

Chang-Sheng Guo,[1, #] Xiaolong Su,[1, #] Mengxin Liu,[1] Pu Chen,[1] Jia-Wen Zhao,[1] Chunxuan Qi,[1] Guogang Shan,[3] Hai-Tao Feng,[1, *] and Ben Zhong Tang[2, *]

[1]AIE Research Center, Shaanxi Key Laboratory of Phytochemistry, College of Chemistry and Chemical Engineering, Baoji University of Arts and Sciences, Baoji 721013, China

[2]School of Science and Engineering, Shenzhen Institute of Aggregate Science and Technology, The Chinese University of Hong Kong, Shenzhen (CUHK-Shenzhen), Shenzhen 518172, China

[3]Institute of Functional Material Chemistry and National & Local United Engineering Lab for Power Battery, Faculty of Chemistry, Northeast Normal University, Changchun 130024, China

Section A. Materials and methods Materials:

All reagents and solvents were chemical pure (CP) grade or analytical reagent (AR) grade and were used as received unless otherwise indicated.

Measurements: ^{1}H NMR and ^{13}C NMR spectra were obtained by an Agilent NMR Systems 400MHz NMR Spectrometer at 298 K. High resolution mass spectra (HRMS) were obtained by use of a Bruker Compact TOF mass spectrometer in electrospray ionization mode (ESI^{+}). Absorption spectra were recorded on a YOKU INSTRUMENT TS2023 UV-Vis spectrophotometer. Fluorescence spectra were collected on a Techcomp FL970 fluorophotometer at 298 K. The luminescence lifetimes were measured on an Edinburgh FLS 1000 fluorescence spectrometer operating in time correlated single-photon counting (TCSPC) mode. Quantum yield was measured using a Hamamatsu C11347 Quantaurus-QY integrating sphere. Particle size and morphology were observed on a FEI Tecnai F20 transmission electron microscope (TEM).

Section B. Experimental details for synthesis and characterization of new compounds.

1 Synthesis of R/S-TPE macrocycle (TPEM)

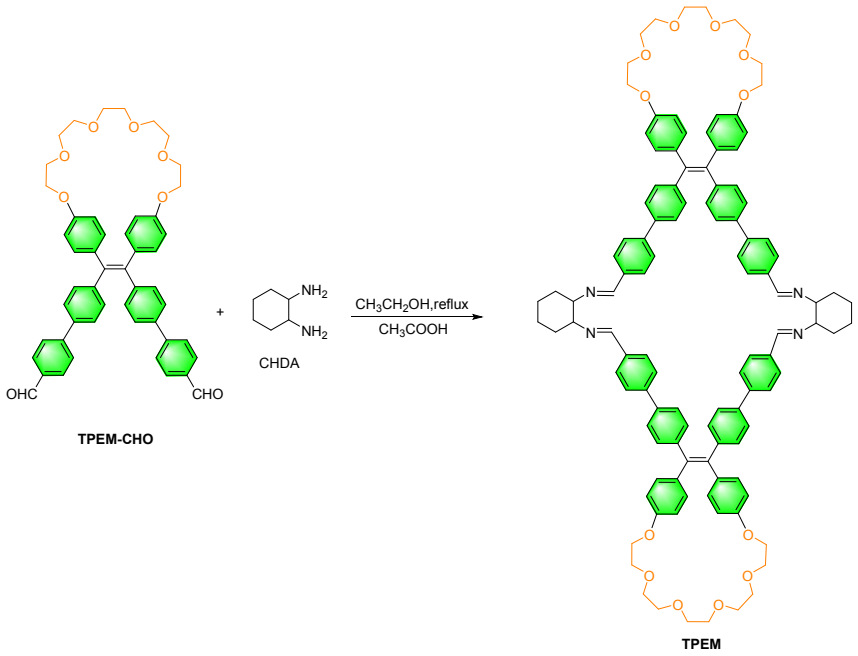

Scheme S1. Synthetic route of TPEM.

Synthesis of TPEM: Compound TPE-CHO is known molecule and synthesized according to previous publication. To a one-neck 50 mL flask, compound TPE-CHO (154.9 mg, 0.2 mmol) and CHDA (25.1 mg, 0.22 mmol) were dissolved in ethanol (20 mL). Then 5 drops of acetic acid were added in the solvent and refluxed for 12 h. The crude product was obtained by filtration. Finally, the crude product was recrystallized in DCM/ethanol mixture (v/v = 1/1) to give green solid (136.5 mg, yield 80%). ^{1}H NMR (400 MHz, $CDCl_3$) δ 8.20 (s, 4H), 7.61 (d, J = 8.0 Hz, 8H), 7.49 (d, J = 8.0 Hz, 8H), 7.32 (d, J = 8.0 Hz, 8H), 7.12 (d, J = 8.0 Hz, 8H), 6.91 (d, J = 8.8Hz, 8H), 6.67 (d, J = 8.8 Hz, 8H), 4.12 – 4.10 (m, 8H), 3.81 – 3.79 (m, 8H), 3.68 – 3.66 (m, 24H), 3.41 – 3.39 (m, 4H), 1.93 – 1.88 (m, 12H), 1.50 (s, 4H). ^{13}C NMR (100 MHz, $CDCl_3$) δ 161.10, 157.34, 143.14, 142.78, 139.94, 138.48, 136.92, 135.32, 132.72, 131.97, 128.40, 127.11, 126.49, 114.23, 73.67, 71.18, 70.80, 70.63, 69.63, 67.80, 33.03, 24.68. ESI^{+} HRMS m/z calcd. for $C_{112}H_{113}N_4O_{12}$ 1706.8383 $[M+H]^+$, found 1706.8366 $[M+H]^+$.

2 Synthesis of PZ

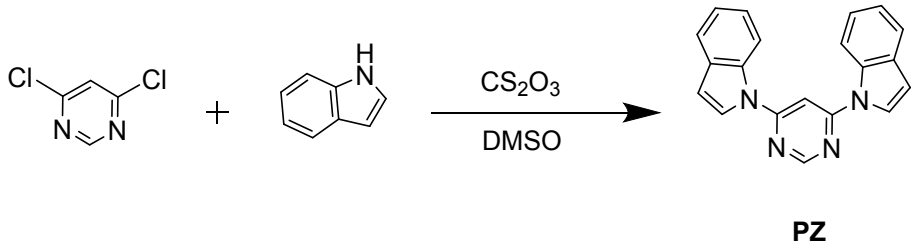

PZ

Scheme S2. Synthetic route of **PZ**

Synthesis of PZ: To a one-neck 50 mL flask, compound 4,6-dichloropyrimidine (0.5 g, 3.36 mmol), Indole (1.2 g, 10.08 mmol) and Cs_2CO_3 (3.2 g, 10.08 mmol) were dissolved in DMSO (25 mL). The mixture solution was reacted at 110 ℃ for 12h. The crude product was purified by column chromatography (silica gel, Ethyl acetate/ petroleum ether 10: 1) to give white solid (0.9 g, 86%). ^{1}H NMR (400 MHz, $CDCl_3$) δ 9.01 (s, 1H), 8.49 (d, J = 8.4 Hz, 2H), 7.83 (d, J = 3.6 Hz, 2H), 7.67 (d, J = 7.6 Hz, 2H), 7.47 (s, 1H), 7.42 – 7.37 (m, 2H), 7.31 – 7.26 (m, 2H), 6.81 (d, J = 3.6 Hz, 2H). ^{13}C NMR (100 MHz, $CDCl_3$) δ 159.47, 158.97, 135.35, 131.24, 124.81, 124.31, 122.72, 121.54, 114.85, 108.40, 96.44.

3. Characteristic Spectra

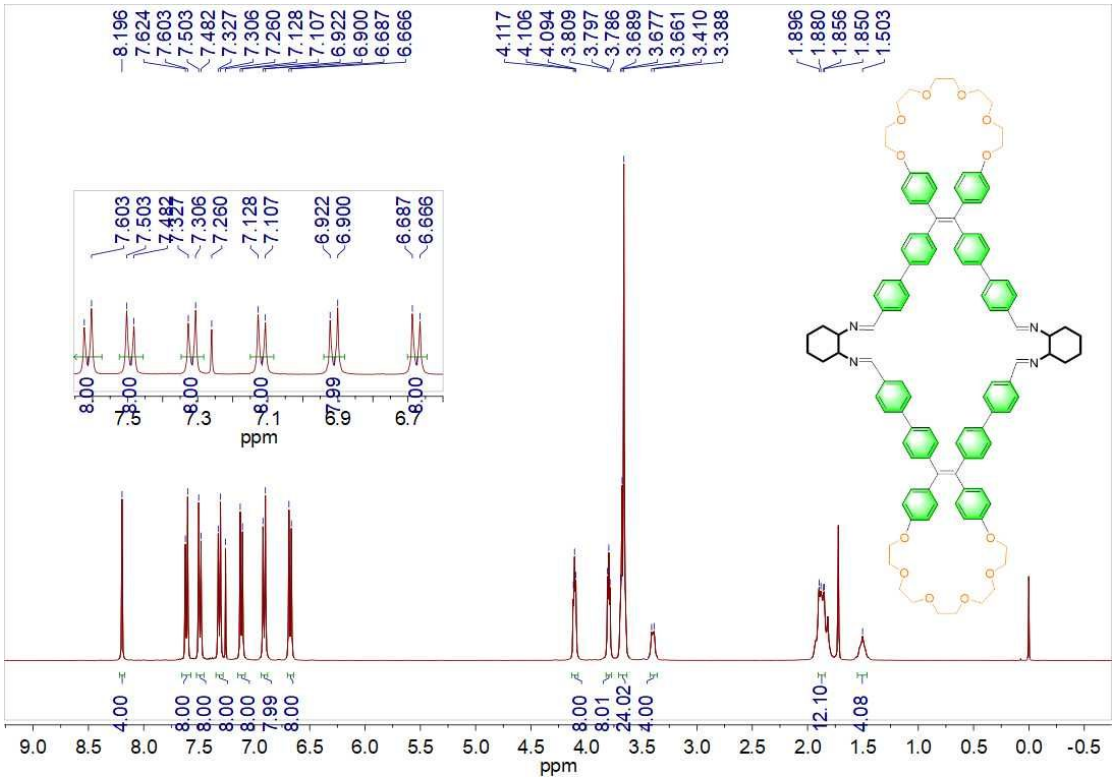

Figure S1. ^{1}H NMR spectra of TPEM (in $CDCl_3$).

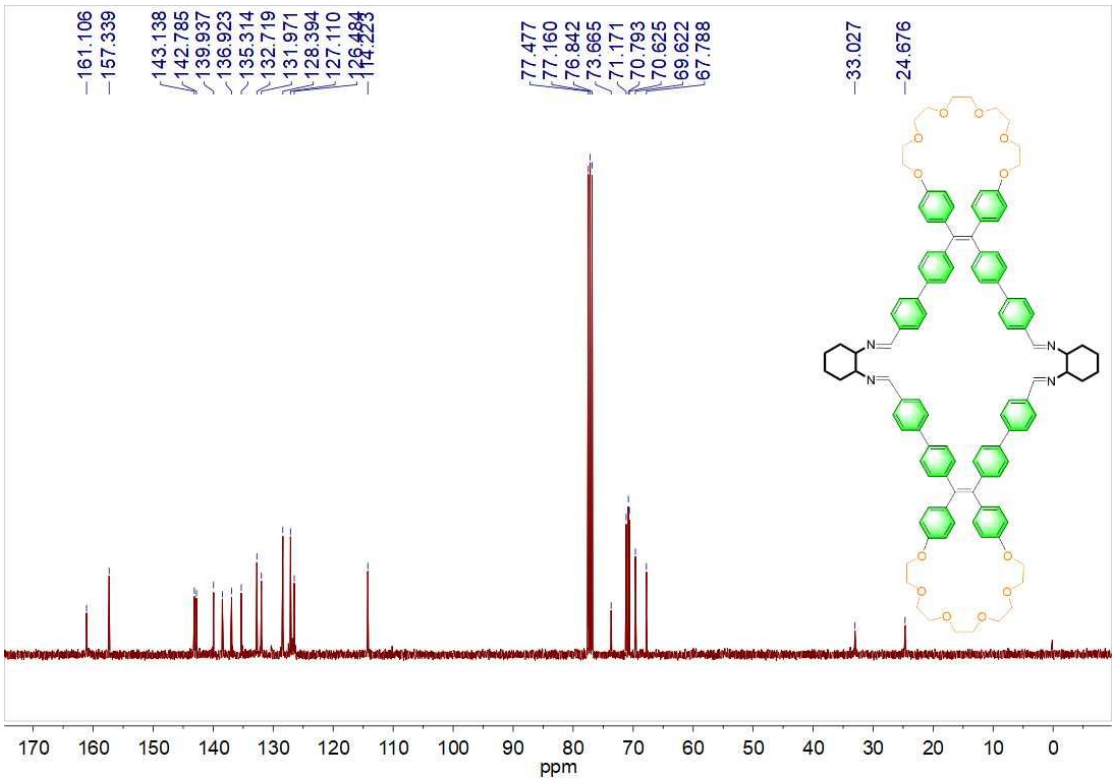

Figure S2. ^{13}C NMR spectra of TPEM (in $CDCl_3$).

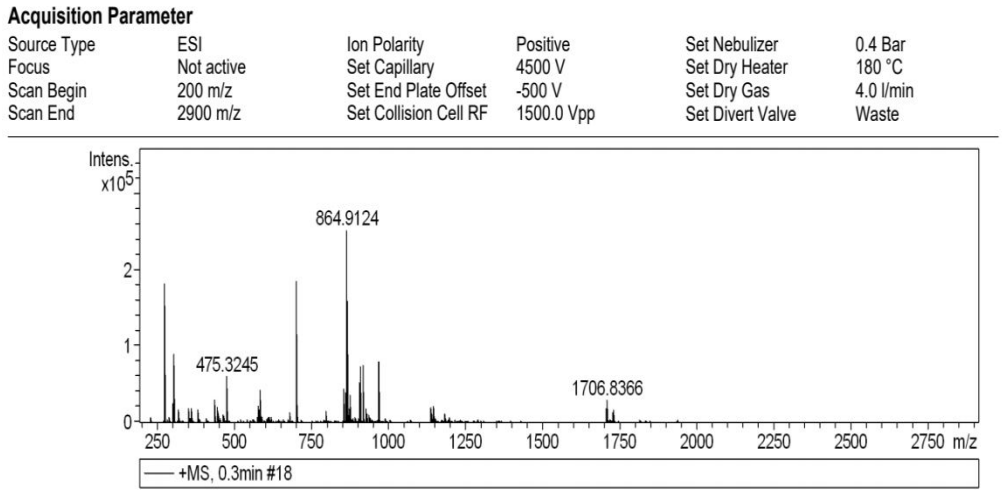

Figure S3. HRMS spectrum of TPEM.

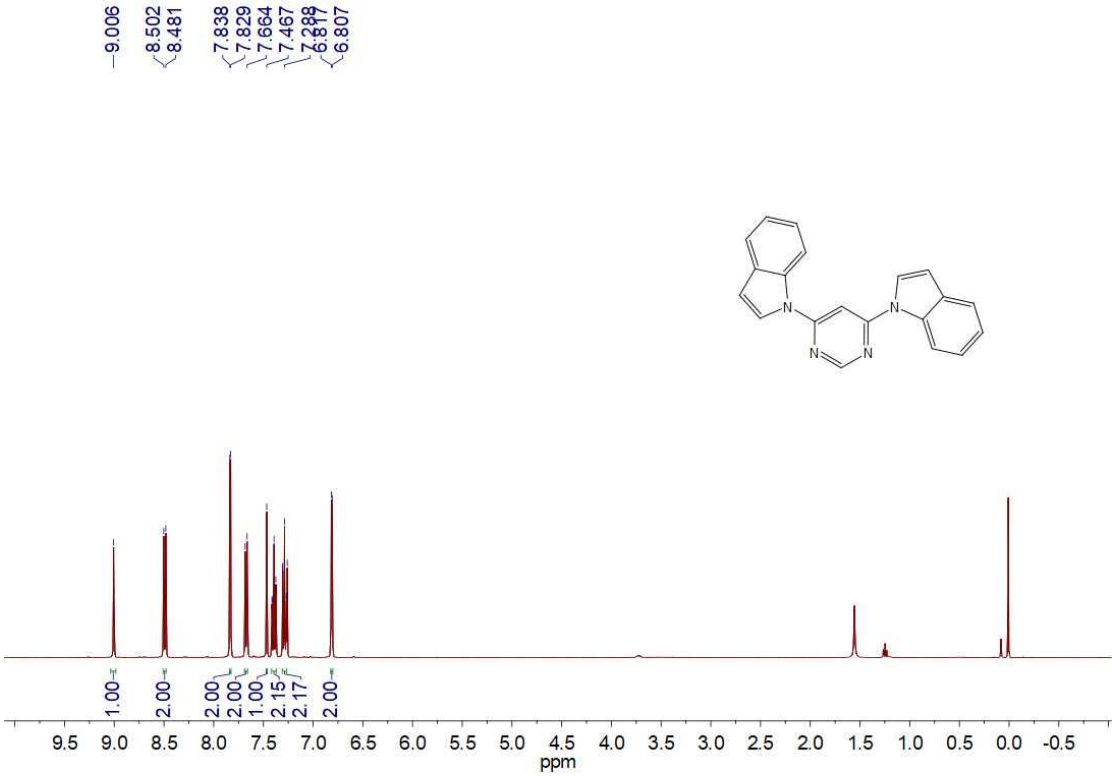

Figure S4. ^{1}H NMR spectra of PZ (in $CDCl_3$).

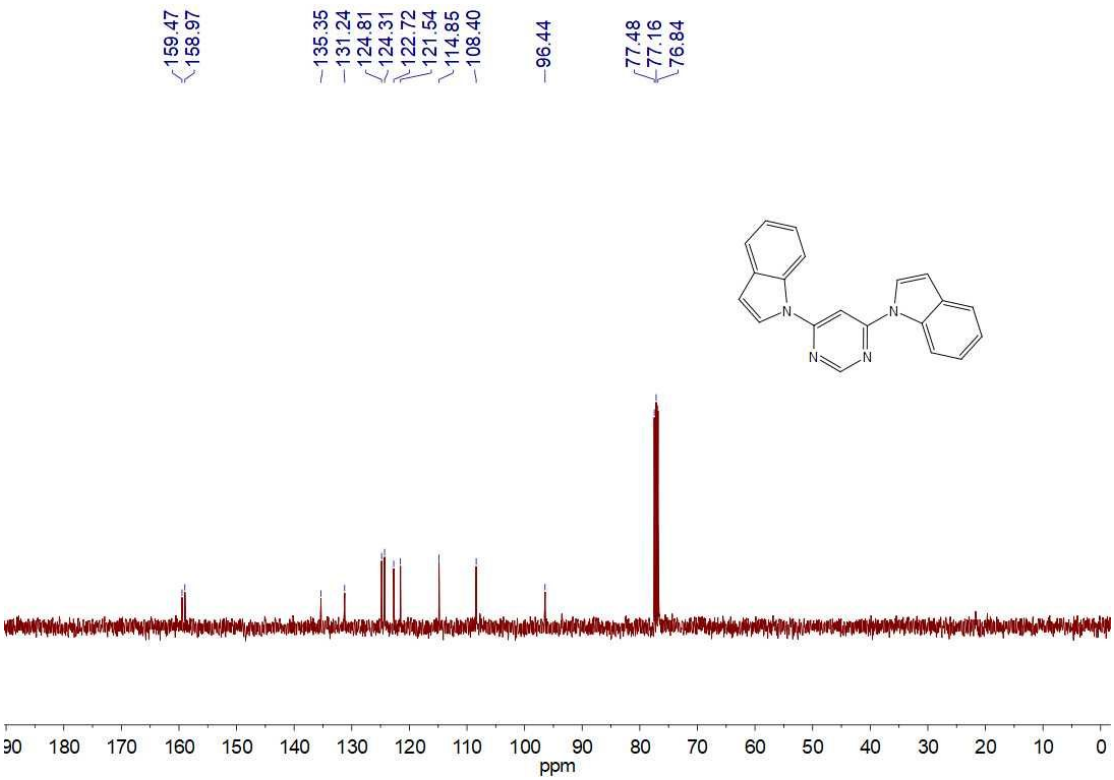

Figure S5. ^{13}C NMR spectra of PZ (in $CDCl_3$).

Section C. Construction of artificial light-harvesting systems

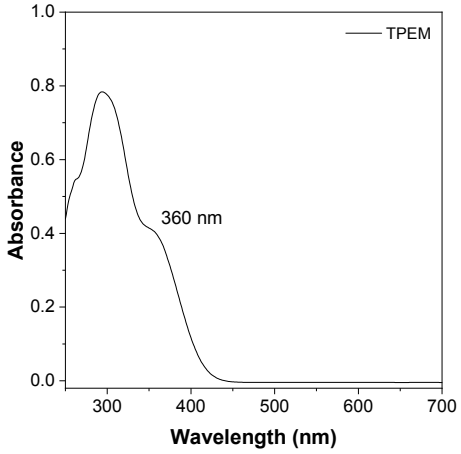

Figure S6. UV-vis spectra of TPEM in THF, c = 1.0×10^{-5} M.

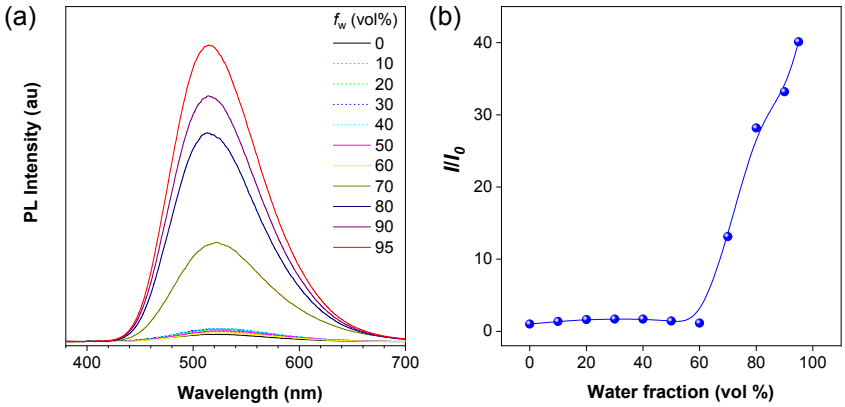

Figure S7. (a) Fluorescence emission spectra of 10 μM TPEM in THF/H_2O with different H_2O fraction, λ_{ex} = 360 nm, c = 1.0×10^{-5} M. (b) Fluorescence intensity of versus H_2O fractions.

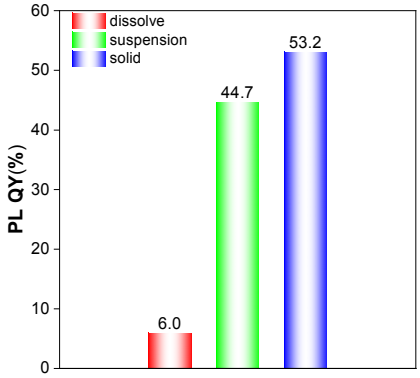

Figure S8. Fluorescence QY of TPEM in THF, 95% water fraction and solid state.

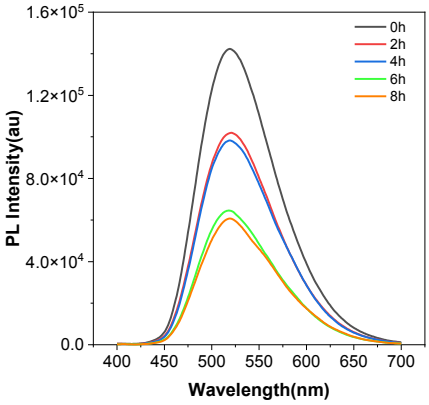

Figure S9. Fluorescence spectra of 10 μM TPEM in THF/H_2O with 95% water fraction, λ_{ex} = 360 nm.

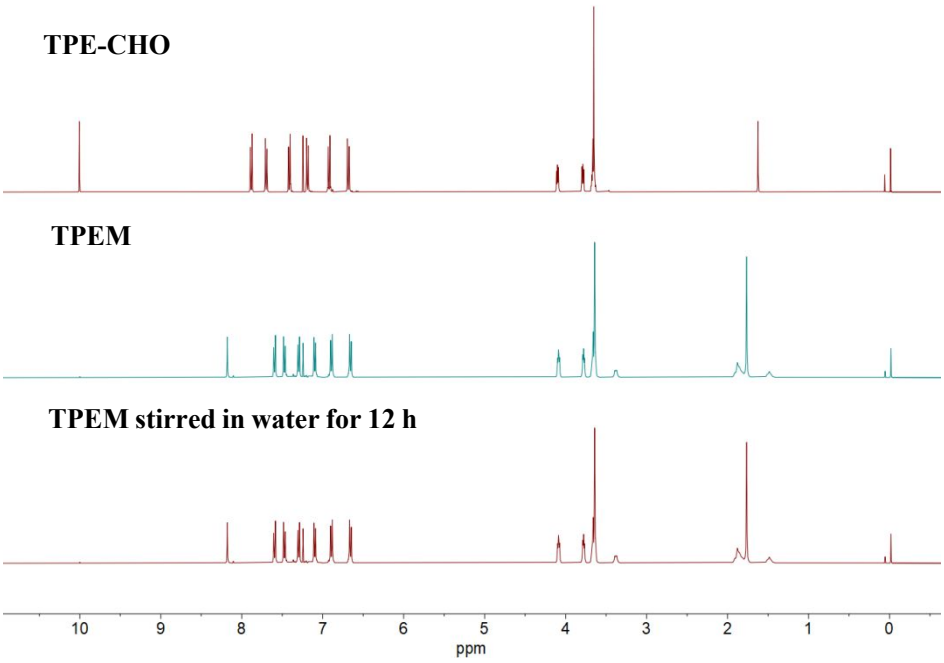

Figure S10. ^1H NMR spectra of TPE-CHO, TPEM, TPEM stirred in water for 12h. (in $CDCl_3$).

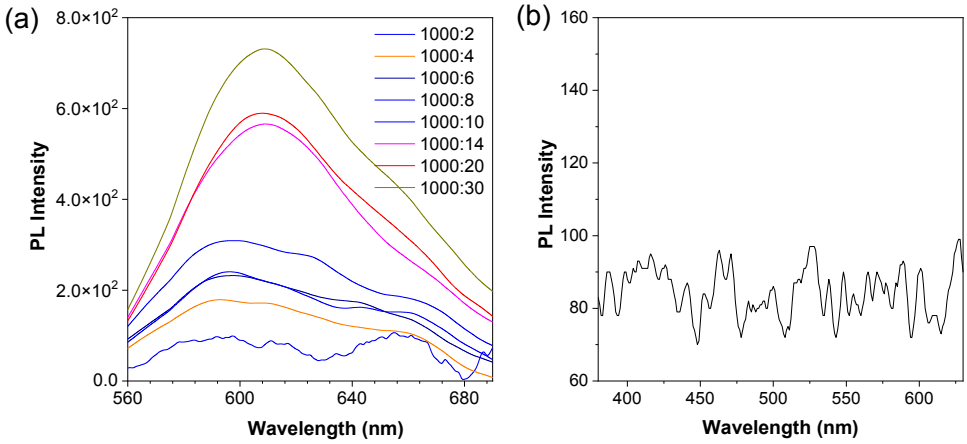

Figure S11. Control experiment. (a) Fluorescence spectra changes of TPEM (10 μM) titrated by NIR (0−0.03 equiv.) in THF/H_2O (1:19, v/v), λex = 532 nm, Ex/Em slit = 2.5/1 nm. (b) Fluorescence spectra of NIR (0.03 equiv.) without TPEM (10 μM) in THF/H_2O (1:19, v/v). λex = 360 nm, Ex/Em slit = 2.5/1 nm.

Energy transfer efficiency (Φ_{ET}) and antenna effect (AE) calculation[S1]

1) Energy transfer efficiency (Φ_{ET}), is the ability to transfer energy from donor to acceptor, that is, the ratio of the fluorescence intensity of the donor in the absence of and presence of the acceptor(I_D and I_{DA}). Φ_{ET} was calculated using Equation S1:

$$\Phi_{ET} = 1-I_{DA}/I_D \quad \textbf{(Eq. S1)}$$

Where I_{DA} and I_D are the fluorescence intensities at 519 nm of **TPEM/NIR** and **TPEM** respectively when excited at 360 nm.

2) Antenna effect (AE), is the ability of the acceptor to harvest energy from the donor. AEwascalculated using Equation S2:

$$AE = (I_{DA,360}-I_{D,360})/I_{DA,532} \quad \textbf{(Eq. S2)}$$

Where $I_{DA,360}$ is the fluorescence intensity at Maximum emission wavelength nm of **TPEM/NIR** when indirect excitation of the acceptor at 360 nm, $I_{D,360}$ is the fluorescence intensity at Maximum emission wavelength nm of **TPEM** which is normalizedwith **TPEM/NIR** at 519 nm. $I_{DA,532}$ is the fluorescence intensity at Maximum emission wavelength of **TPEM/NIR** when direct excitation of the acceptor at 532 nm.

Table S2 Φ_{ET} and AE calculation of TPEM/NIR in THF/H_2O (1:19, v/v)

TPEM/NIR	$I_{DA}(I_D)$	I_{DA360}	I_{D360}	I_{DA532}	Φ_{ET}/%	*AE*
1000:0	74071	--	--	--	--	--
1000:2	39621	31108	16869	87	46.51	163.67
1000:4	24128	28524	5439	178	67.43	107.56
1000:6	15415	25305	3475	232	79.19	85.72
1000:8	11675	24149	2632	240	84.24	84.11
1000:10	7952	20478	1793	309	89.26	57.60
1000:14	5968	19786	1345	551	91.94	32.62
1000:20	3813	16502	860	582	94.85	26.49
1000:30	1154	8900	260	730	98.44	11.84

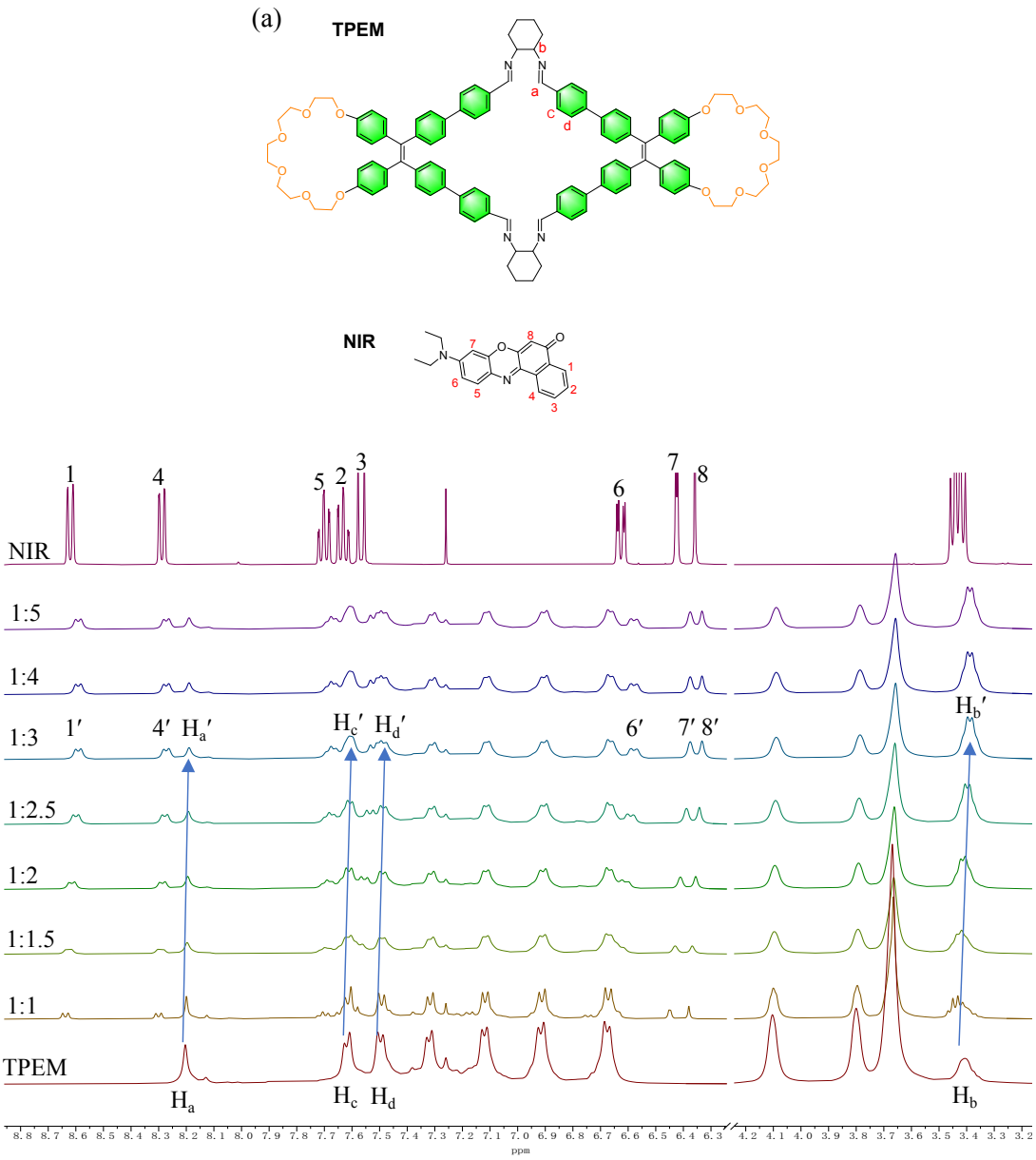

Figure S12. The host-guest investigations of TPEM-NIR. (a) The chemical structure of TPEM and NIR. (b) Part of ^{1}H NMR spectra (400 MHz, $CDCl_3$) of TPEM (1.0 mM) titrated with NIR (0-5.0 equiv.). Here, primes (') denote the resonances of the TPEM-NIR inclusion complex.

In addition, the proton resonances of NIR were downshielded upon mixing with TPEM as compared to the ^{1}H NMR spectrum of NIR, where electron-withdrawing C = N bond of TPEM could contribute to the deshielding effect in NIR.

Table S2 ^{1}H NMR chemical shift changes upon titration of compounds TPEM and NIR

Chemical shift	H1	H4	H6	H7	H8	H_a	H_b	H_c	H_d
From	8.61	8.30	6.61	6.42	6.36	8.18	3.37	7.60	7.48

To	8.58	8.27	6.56	6.37	6.33	8.20	3.42	7.62	7.49
Δδ/ppm	0.03	0.03	0.05	0.05	0.03	-0.02	-0.05	-0.02	-0.01

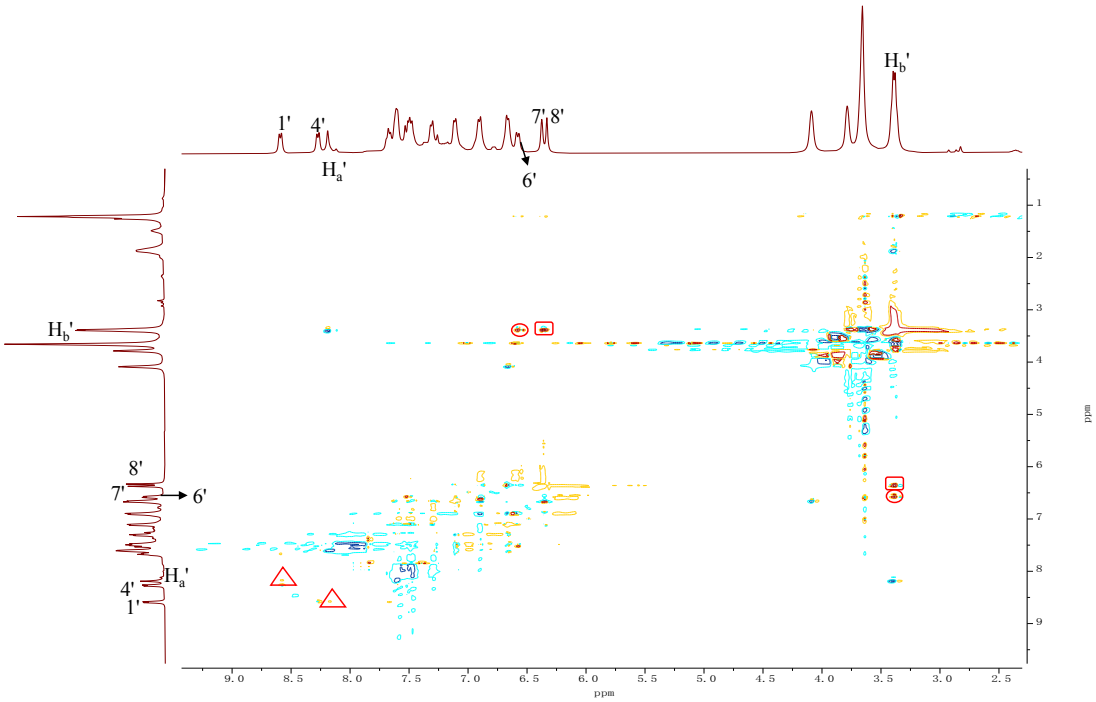

Figure S13. Partial 2D NMR NOESY (400 MHz) spectra of TPEM and NIR in $CDCl_3$. [TPEM] = 1.0 mmol/L, [NIR] = 3.0 mmol/L. The red cycles and geometric shapes indicated the cross-peaks.

In the 2D NMR NOESY spectrum of TPEM-NIR complex in $CDCl_3$, obvious symmetrical cross peaks are observed for protons H1-H_a, H6-H_b (labeling of protons as in Figure S12) demonstrating those protons are close to each other. In addition, proton H7 of NIR, which showed obvious cross-peak with H8 of NIR because they were close to each other, displayed NOE signals with protons Hb of TPEM, suggesting that the π-electron-rich aromaticity of NIR and the double bound with C = N-bond of TPEM were very close. The observed correlations in 2D NMR NOESY spectrum of TPEM-NIR complex clearly shows NIR is encapsulated into the cavity of TPEM.

Table S3 Fluorescence lifetimes of TPEM/NIR in THF/H_2O (1:19, v/v) monitored at 518 nm

TPEM/NIR	τ_1	τ_2	α_1	α_2	τ_{ave}	$\chi 2$
1000:0	3.64	7.08	46.41%	53.59%	5.48	1.22
1000:10	1.87	6.00	80.32%	19.68%	2.68	1.26
1000:20	0.52	2.06	22.01%	77.99%	1.72	1.36
1000:30	0.37	1.87	48.05%	51.95%	1.07	1.48

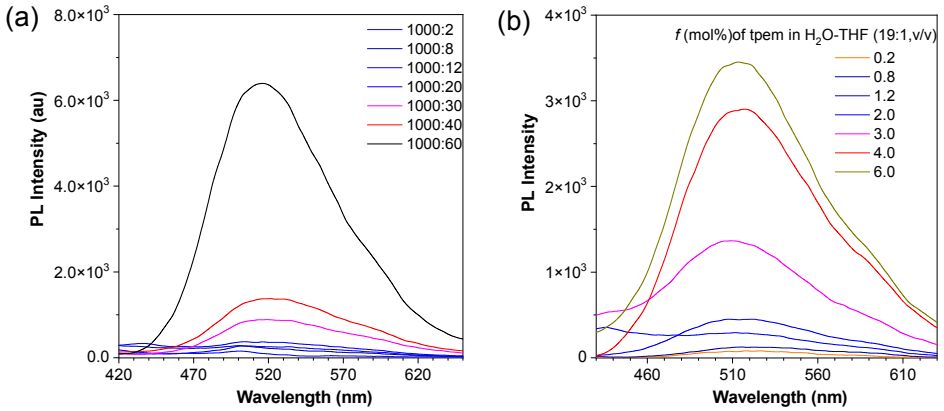

Figure S14. Control experiment. (a) PL spectra changes of PZ (10 μM) titrated by TPEM (0−0.03 equiv.) in THF/H_2O (1:19, v/v), λex = 360 nm, Ex/Em slit = 2.5/1. (b) PL spectra of TPEM (0-0.06 equiv.) without PZ (10 μM) in THF/H_2O (1:19, v/v). λex = 323 nm, Ex/Em slit = 2.5/1.

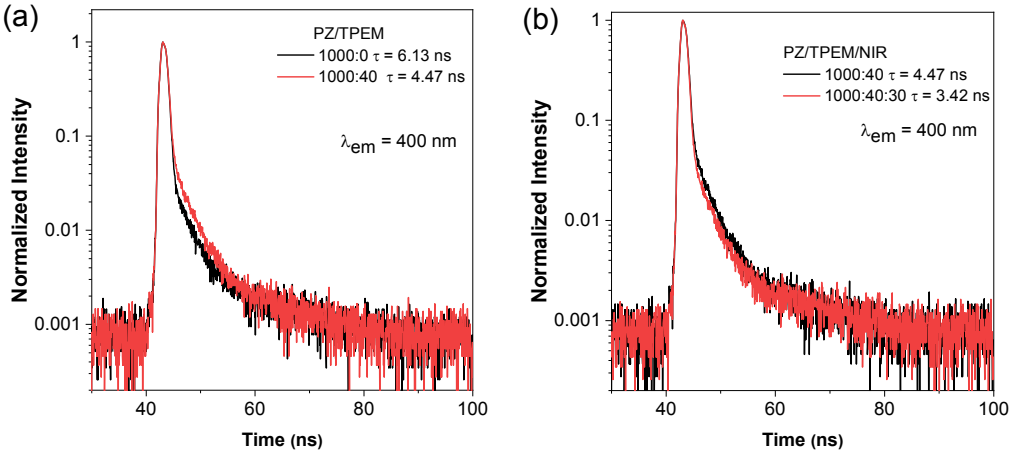

Figure S15. Fluorescence decay profiles of (a) PZ at 400 nm in the absence and presence of TPEM, solution: THF/H_2O = 1:19, (v/v). (b) PZ/TPEM at 400 nm in the absence and presence of NIR, solution: THF/H_2O = 1:19, (v/v).

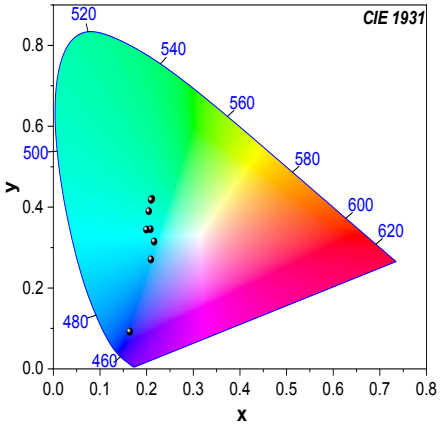

Figure S16. CIE 1931 chromaticity coordinates changes of PZ (10 μM) with different doses of TPEM (λex = 323 nm, Ex/Em slit = 2.5/1).

Energy transfer efficiency (Φ_{ET}) and antenna effect (AE) calculation[S1-S3]

1) Energy transfer efficiency (Φ_{ET}), is the ability to transfer energy from donor to acceptor, that is, the ratio of the fluorescence intensity of the donor in the absence of and presence of the acceptor (I_D and I_{DA}). Φ_{ET} was calculated using Equation S1:

$$\Phi_{ET} = 1\text{-}I_{DA}/I_D$$

Where I_{DA} and I_D are the fluorescence intensities at 400 nm of **PZ/TPEM** and **PZ** respectively when excited at 323 nm.

2) Antenna effect (AE), is the ability of the acceptor to harvest energy from the donor. AE was calculated using Equation S2:

$$AE = (I_{DA,323}\text{-}I_{D,323})/I_{DA,360}$$

Where $I_{DA,323}$ is the fluorescence intensity at Maximum emission wavelength nm of **PZ/TPEM** when indirect excitation of the acceptor at 323 nm, $I_{D,323}$ is the fluorescence intensity at Maximum emission wavelength nm of **PZ** which is normalized with **PZ/TPEM** at 400 nm. $I_{DA,360}$ is the fluorescence intensity at Maximum emission wavelength of TPEM/NiR when direct excitation of the acceptor at 360 nm.

Table S4 Φ_{ET} and AE calculation of PZ/TPEM in THF/H_2O (1:19, v/v)

PZ/TPEM	$I_{DA}(I_D)$	I_{DA323}	I_{D323}	I_{DA360}	Φ_{ET}/%	*AE*
1000:0	35260	--	--	--	--	--
1000:2	26751	15023	4226	150	24.13	71.98
1000:8	20154	18891	3123	262	42.84	78.06
1000:12	10909	28321	1839	267	69.06	99.18
1000:20	7084	34802	1399	303	79.91	110.24
1000:30	3734	39255	649	704	89.41	54.84
1000:40	2136	45847	341	1158	93.94	39.30
1000:60	1262	58234	202	5792	96.42	10.02

Energy transfer efficiency (Φ_{ET}) and antenna effect (AE) calculation[S1-S3]

1) Energy transfer efficiency (Φ_{ET}), is the ability to transfer energy from donor to acceptor, that is, the ratio of the fluorescence intensity of the donor in the absence of and presence of the acceptor (I_D and I_{DA}). Φ_{ET} was calculated using Equation S1:

$$\Phi_{ET} = 1\text{-}I_{DA}/I_D$$

Where I_{DA} and I_D are the fluorescence intensities at 400 nm of **PZ/TPEM/NIR** and **PZ/TPEM** respectively when excited at 323 nm.

2) Antenna effect (AE), is the ability of the acceptor to harvest energy from the donor. AE was calculated using Equation S2:

$$\mathbf{AE = (I_{DA,323}-I_{D,323})/I_{DA,532}}$$

Where $I_{DA,323}$ is the fluorescence intensity at Maximum emission wavelength nm of **PZ/TPEM /NIR** when indirect excitation of the acceptor at 323 nm, $I_{D,323}$ is the fluorescence intensity at Maximum emission wavelength nm of **PZ/TPEM** which is normalized with **PZ/TPEM/NIR** at 5 nm. $I_{DA,360}$ is the fluorescence intensity at Maximum emission wavelength of **PZ/TPEM/NIR** when direct excitation of the acceptor at 498 nm.

Table S5 Φ_{ET} and AE calculation of **PZ/TPEM/NIR** in THF/H_2O (1:19, v/v)

PZ/TPEM/NIR	$I_{DA}(I_D)$	I_{DA323}	I_{D323}	I_{DA360}	Φ_{ET}/%	*AE*
1000:40:0	45304	--	--	--	--	--
1000:40:2	32510	14579	7439	150	28.24	47.60
1000:40:4	26862	18551	4780	124	40.71	111.06
1000:40:8	14403	18755	2193	149	68.21	111.15
1000:40:12	6538	17281	847	151	85.57	108.83
1000:40:20	3948	17666	506	159	91.29	107.92
1000:40:30	639	17222	41	454	98.59	37.84

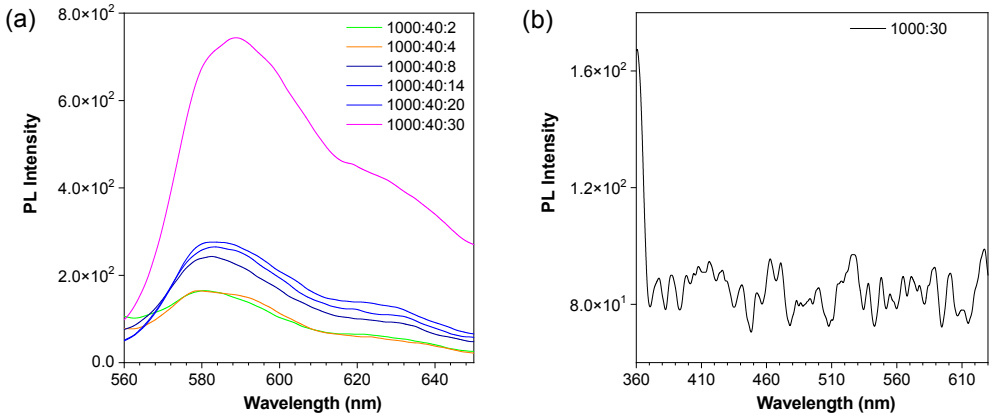

Figure S17. (a) Fluorescence spectra changes of PZ/TPEM (10 μM, 1000:40) titrated by NIR (0−0.03 equiv.) in THF/H_2O (1:19, v/v), λ_{ex} = 532 nm, Ex/Em slit = 2.5/1. (b) Fluorescence spectra of NIR (0.03 equiv.) and PZ (10 μM) without TPEM in THF/H_2O (1:19, v/v). λ_{ex} = 532 nm, Ex/Em slit = 2.5/1.

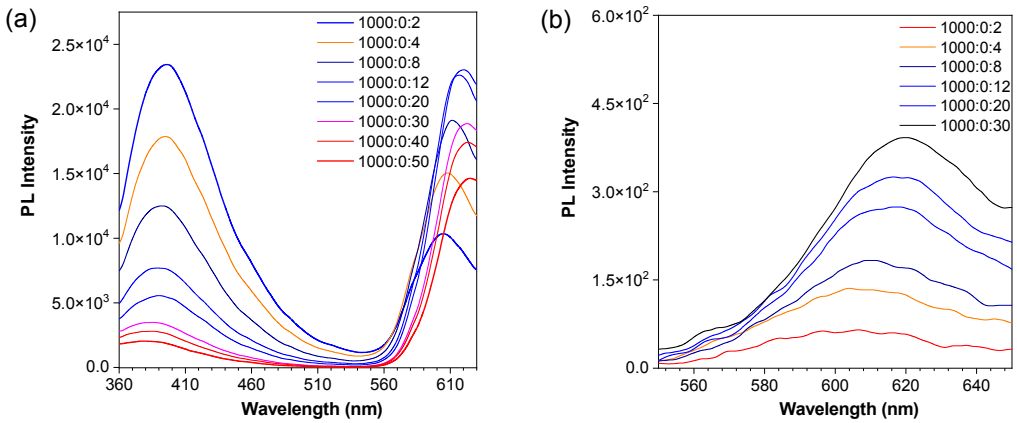

Figure S18. PZ (10 μM) without TPEM titrated by NIR (0−0.03 equiv.) in THF/H_2O (1:19, v/v) (a) λ_{ex} =323 nm, (b) λ_{ex} =532 nm, Ex/Em slit = 2.5/1.

Table S6. QY of the co-assembled system.

Sample	Condition	QY
PZ	THF/H_2O (1:19, v/v), c = 1 × 10^{-5} M	7.6%
PZ/TPEM	THF/H_2O (1:19, v/v), c = 1 × 10^{-5} M	20.2%
PZ/TPEM/NIR	THF/H_2O (1:19, v/v), c = 1 × 10^{-5} M	27.3%

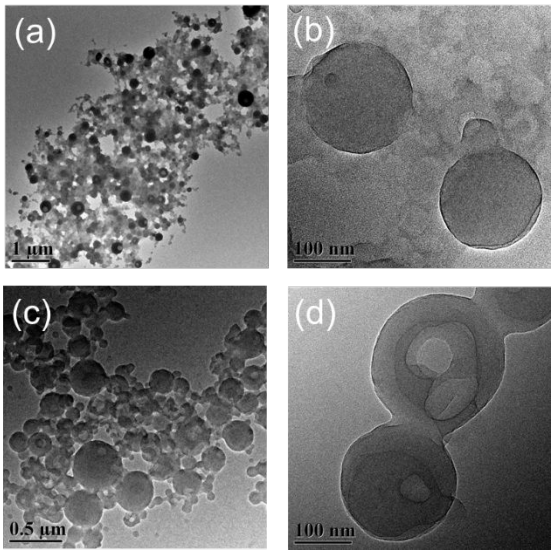

Figure S19. TEM images of (a-b) TPEM, (c-d) TPEM/NIR (1000:30) in THF/H_2O (1:19, v/v).

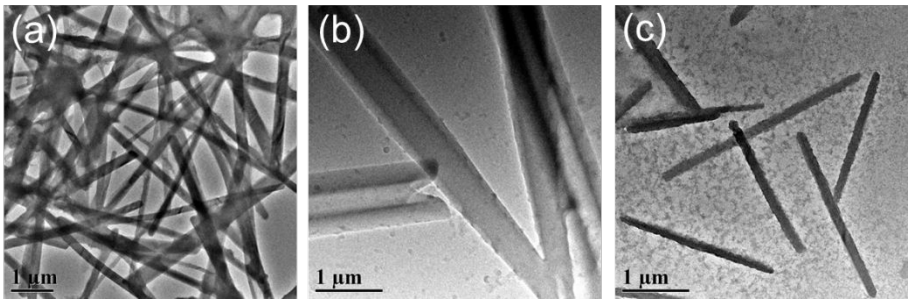

Figure S20. TEM images of (a) PZ in THF/H_2O (1:19, v/v); (b) PZ/TPEM (1000:40, molar ratio), (c) PZ/TPEM/NIR (1000:40:30) in THF/H_2O (1:19, v/v).

Section D. Investigation of the photocatalytic activity of the light harvesting systems.

Photocatalytic Knoevenagel condensation reaction:

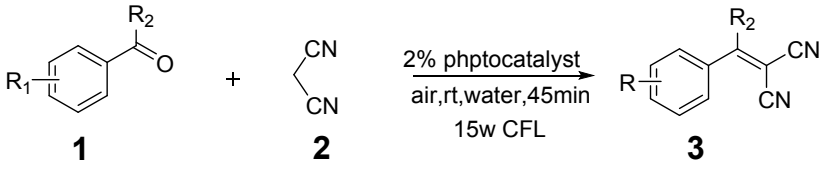

Table S7 Control experiments for Knoevenagel condensation

Entry	Conditions	Notes	Yield[a][%]
1	Dark	Importance of light	21
2	No catalyst	Importance of catalyst	39
3	N_2	Importance of oxygen	13
4	TEMPO	Radical scavenger of all	54
5	BHT	Radical scavenger of all	25
6	Benzoquinone	$O_2^{\cdot-}$ scavenger	88
7	KI	H^+ scavenger	79
8	Isopropanol	·OH scavenger	30
7	β-carotene	$^1O_2$ scavenger	14

[a] Isolated yield.

Synthetic procedure:

An oven-dried glass vial was charged with aldehyde/ketone **1** (0.94 mmol), compound **2** (1.88 mmol), PZ 5.8mg, TPEM 1.3mg, NIR 57 μL (c = 1.0×10^{-2} M, solvent: THF) 4 mL distilled water/ EtOH was added to the reaction mixture and the glass vial was irradiated with 15 W CFL light for 45 min. (in case of aldehydes) or 24 h (in the case of ketones). The progress of the reaction was monitored by TLC. After completion of the reaction, 10 mL of distilled water was added to the reaction mixture. precipitation appeared. The precipitation was filtered to get solid. In case of aldehydes. It was washed

several times with water and one to two times with Water: EtOH (2:1) to get pure product. In the case of ketones. It was washed several times with Water: EtOH (1:1).

3a (2-benzylidenemalononitrile) 95% yield; ^{1}H NMR (400 MHz, $CDCl_3$) δ 7.92 – 7.89 (m, 2H), 7.78 (s, 1H), 7.65 – 7.61 (m, 1H), 7.56 – 7.52 (m, 2H). ^{13}C NMR (100 MHz, $CDCl_3$) δ 160.04, 134.74, 131.07, 130.84, 129.76, 113.81, 112.65, 83.06.

3b (2-(2-bromobenzylidene)malononitrile) 78% yield; ^{1}H NMR (400 MHz, $CDCl_3$) δ 8.22 (s, 1H), 8.14 – 8.11 (m, 1H), 7.76 – 7.73 (m, 1H), 7.52 – 7.43 (m, 2H). ^{13}C NMR (100 MHz, $CDCl_3$) δ 158.84, 135.07, 134.14, 130.96, 129.96, 128.48, 126.58, 113.24, 111.92, 86.23.

3c (2-(4-bromobenzylidene)malononitrile) 83% yield; ^{1}H NMR (400 MHz, $CDCl_3$) δ 7.78 – 7.76 (m, 2H), 7.71 (s, 1H), 7.70 – 7.67 (m, 2H). ^{13}C NMR (100 MHz, $CDCl_3$) δ 158.53, 133.22, 131.93, 130.05, 129.80, 113.57, 112.45, 83.69.

3d (2-(4-fluorobenzylidene)malononitrile) 68% yield; ^{1}H NMR (400 MHz, $CDCl_3$) δ 7.98 – 7.95 (m, 2H), 7.75(s, 1H), 7.27 – 7.22 (m, 2H). ^{13}C NMR (100 MHz, $CDCl_3$) δ 166.26 (d, J = 259 Hz), 158.38, 133.55 (d, J = 9.5 Hz), 127.51 (d, J = 3.3 Hz), 117.35 (d, J = 22 Hz) , 113.67, 112.61, 82.64 (d, J = 2.6 Hz). ^{19}F NMR (100 MHz, $CDCl_3$) δ -100.11.

3e (2-(4-chlorobenzylidene)malononitrile) 96% yield; ^{1}H NMR (400 MHz, $CDCl_3$) δ 7.85 (d, J = 8.8 Hz, 2H), 7.73 (s, 1H), 7.52 (d, J = 8.8 Hz, 2H). ^{13}C NMR (100 MHz, $CDCl_3$) δ 158.40, 141.24, 131.94, 130.17, 129.40, 113.55, 112.45, 83.47.

3f (2-(4-methylbenzylidene)malononitrile) 85% yield; ^{1}H NMR (400 MHz, $CDCl_3$) δ 7.81 (d, J = 8.0 Hz, 2H), 7.72 (s, 1H), 7.34 (d, J = 8.0 Hz, 2H), 2.46 (s, 3H). ^{13}C NMR (100 MHz, $CDCl_3$) δ 159.85, 146.48, 131.03, 130.50, 128.61, 114.13, 112.97, 81.40, 22.14.

3g (2-(4-(tert-butyl)benzylidene)malononitrile) 75% yield; ^{1}H NMR (400 MHz, $CDCl_3$) δ 7.87 – 7.85 (m, 2H), 7.73 (s, 1H), 7.57 – 7.54 (m, 2H), 1.35 (s, 9H). ^{13}C NMR (100 MHz, $CDCl_3$) δ 159.76, 159.38, 130.97, 128.55, 126.82, 114.15, 112.98, 81.55, 35.68, 31.02.

3h (2-(4-methoxybenzylidene)malononitrile) 94% yield; ^{1}H NMR (400 MHz, $CDCl_3$) δ 7.92 – 7.90 (m, 2H), 7.65 (s, 1H), 7.03 – 6.99 (m, 2H), 3.91 (s, 3H). ^{13}C NMR (100 MHz, $CDCl_3$) δ 164.95, 158.96, 133.57, 124.17, 115.27, 114.54, 113.46, 78.74, 55.93.

3i (2-(4-(dimethylamino)benzylidene)malononitrile) 87% yield; ^{1}H NMR (400 MHz, $CDCl_3$) δ 7.82 – 7.78 (m, 2H), 7.44 (s, 1H), 6.69 (d, J = 9.2 Hz, 2H), 3.14 (s, 6H). ^{13}C NMR (100 MHz, $CDCl_3$) δ 158.18, 154.37, 133.90, 119.43, 116.09, 115.02, 111.74, 72.06, 40.20.

3j (2-(4-(diethylamino)benzylidene)malononitrile) 90% yield; ^{1}H NMR (400 MHz, $CDCl_3$) δ 7.79 (d, J = 8.8 Hz, 2H), 7.43 (s, 1H), 6.67 (d, J = 9.2 Hz, 2H), 3.47 (q, J = 7.2 Hz, 4H), 1.24 (t, J = 7.2 Hz, 6H). ^{13}C NMR (100 MHz, $CDCl_3$) δ 157.90, 152.42, 134.26, 119.18, 116.26, 115.19, 111.60, 71.51, 45.16, 12.65.

3k (2-(naphthalen-1-ylmethylene)malononitrile) 92% yield; ^{1}H NMR (400 MHz, $CDCl_3$) δ 8.65 (s, 1H), 8.27 (d, J = 7.6 Hz, 1H), 8.11 (d, J = 8.4 Hz, 1H), 7.97 – 7.95 (m, 2H), 7.71 – 7.67 (m, 1H), 7.66 – 7.59 (m, 2H). ^{13}C NMR (100 MHz, $CDCl_3$) δ 157.78, 135.03, 133.67, 131.20, 129.55, 128.68,128.62, 127.64, 127.41, 125.50, 122.42, 113.83, 112.61, 85.33.

3l (2-(naphthalen-2-ylmethylene)malononitrile) 90% yield; ^{1}H NMR (400 MHz, $CDCl_3$) δ 8.27 (s, 1H), 8.07-8.05 (m, 1H), 7.96 – 7.88 (m, 4H), 7.70 – 7.66 (m, 1H), 7.63 – 7.59 (m, 1H). ^{13}C NMR (100 MHz, $CDCl_3$) δ 159.81, 135.99, 134.54, 132.73, 130.09, 129.78,129.77, 128.66, 128.14, 127.84, 124.32, 114.11, 112.97, 82.38.

3m (2-(4-(diphenylamino)benzylidene)malononitrile) 76 % yield; ^{1}H NMR (400 MHz, $CDCl_3$) δ 7.73 (d, J = 8.8 Hz, 2H), 7.51 (s, 1H), 7.38 (t, J = 7.8 Hz, 4H), 7.25 – 7.18 (m, 6H), 6.94 (d, J = 8.8 Hz, 2H). ^{13}C NMR (100 MHz, $CDCl_3$) δ 158.03, 153.61, 145.28, 133.12, 130.10 126.86, 126.27, 122.93, 118.62, 115.33, 114.22, 75.70.

3n (2,2'-(1,3-phenylenebis(methanylylidene))dimalononitrile) 90 % yield; ^{1}H NMR (400 MHz, $CDCl_3$) δ 8.21 – 8.18 (m, 2H), 7.84 (s, 2H), 7.77 (t, J = 7.6 Hz, 1H). ^{13}C NMR (100 MHz, $CDCl_3$) δ 157.64, 134.69, 132.48, 132.27, 131.22, 112.89, 111.96, 86.33.

3o (2-(thiophen-2-ylmethylene)malononitrile) 73% yield; ^{1}H NMR (400 MHz, $CDCl_3$) δ 7.89 – 7.87 (m, 2H), 7.82 – 7.80 (m, 1H), 7.29 – 7.26 (m, 1H). ^{13}C NMR (100 MHz,

$CDCl_3$) δ 151.17, 138.23, 136.99, 135.53, 129.15, 113.89, 113.06, 78.53.

3p (2-(1-phenylethylidene)malononitrile) 70% yield; ^{1}H NMR (400 MHz, $CDCl_3$) δ 7.58 – 7.48 (m, 5H), 2.64 (s, 3H). ^{13}C NMR (100 MHz, $CDCl_3$) δ 175.55, 136.05, 132.39, 129.25, 127.46, 112.90,12.82, 84.90, 24.40.

3q (2-(1-(4-fluorophenyl)ethylidene)malononitrile) 77% yield; ^{1}H NMR (400 MHz, $CDCl_3$) δ 7.62 – 7.56 (m, 2H), 7.23 – 7.16 (m, 2H), 2.63 (s, 3H). ^{13}C NMR (100 MHz, $CDCl_3$) δ 173.96, 165.00 (d, J = 254 Hz), 132.03 (d, J = 3.4 Hz), 130.03 (d, J = 9.0 Hz), 116.64 (d, J = 22 Hz), 112.87,112.71, 84.91 (d, J = 1.1 Hz), 24.39. ^{19}F NMR (100 MHz, $CDCl_3$) δ -105.56 (s).

3r (2-(1-(4-chlorophenyl)ethylidene)malononitrile) 75% yield; ^{1}H NMR (400 MHz, $CDCl_3$) δ 7.53 – 7.46 (m, 4H), 2.62 (s, 3H). ^{13}C NMR (100 MHz, $CDCl_3$) δ 173.94, 138.84, 134.27, 129.64, 128.89, 112.68.12.58, 85.31, 24.29.

3s (2-(1-(4-bromophenyl)ethylidene)malononitrile) 71% yield; ^{1}H NMR (400 MHz, $CDCl_3$) δ 7.69 – 7.62 (m, 2H), 7.45 – 7.39 (m, 2H), 2.62 (s, 3H). ^{13}C NMR (100 MHz, $CDCl_3$) δ 174.01, 134.74, 132.64, 128.98, 127.26, 112.66 ,112.57, 85.36, 24.25.

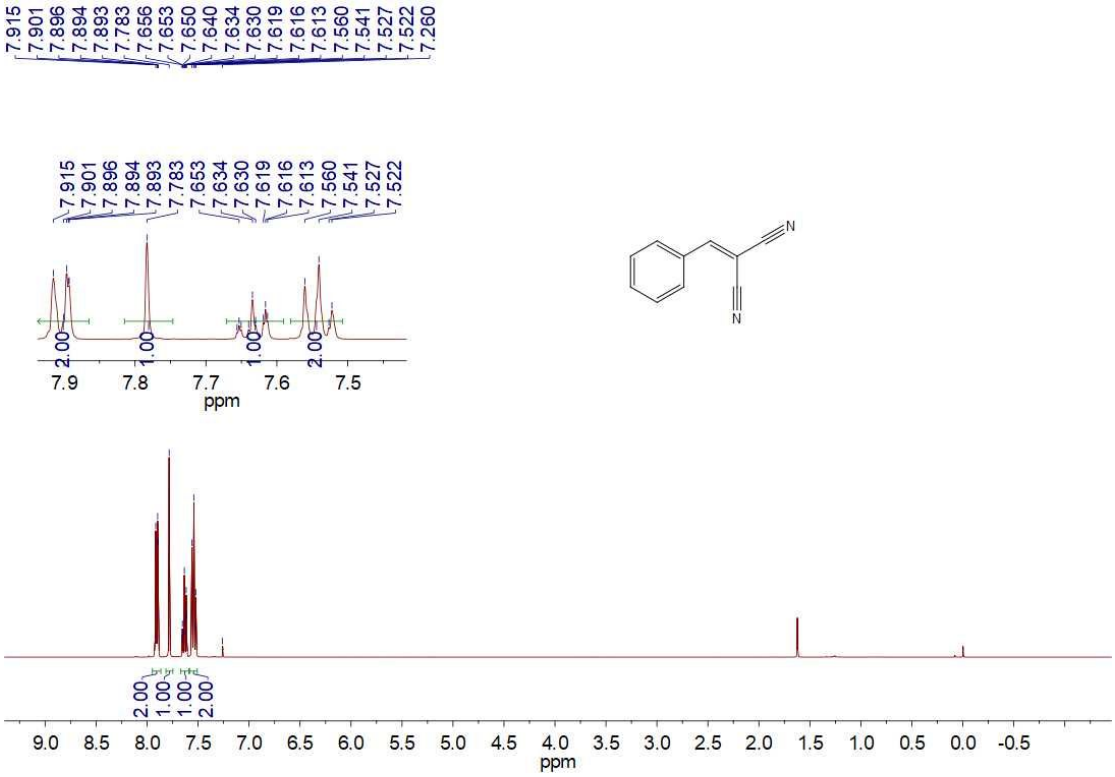

Figure S21. ^{1}H NMR spectra of **3a** (in $CDCl_3$).

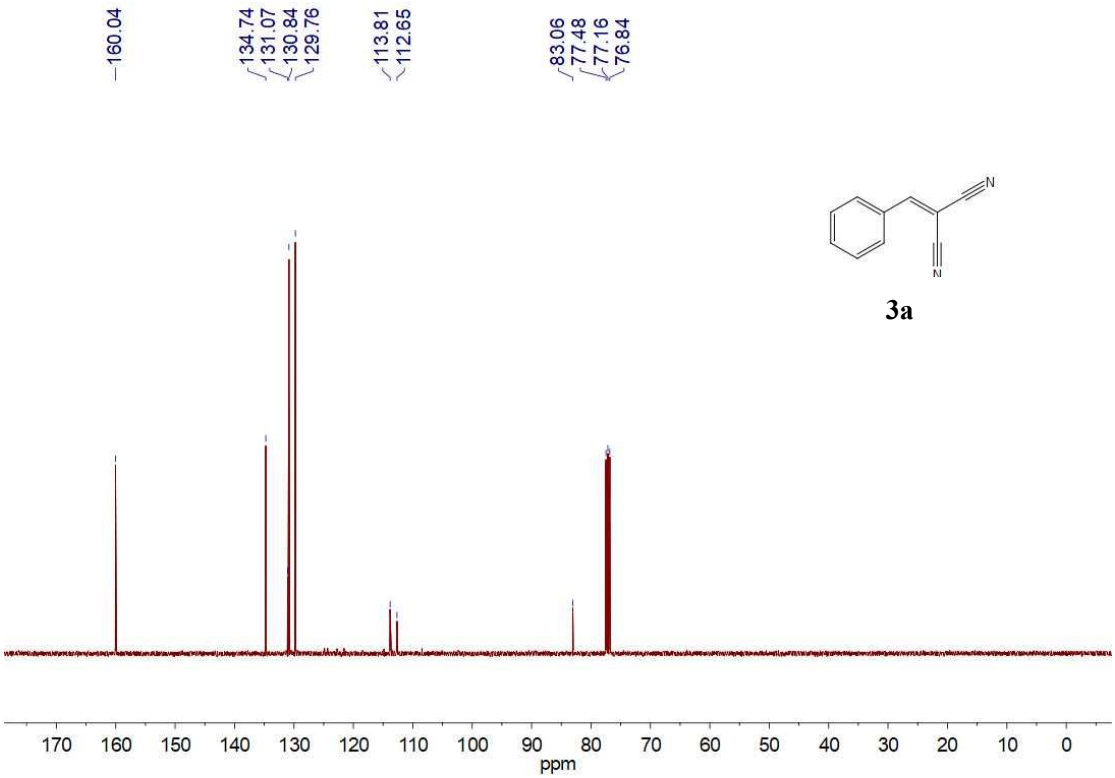

Figure S22. ^{13}C NMR spectrum of **3a** (in $CDCl_3$).

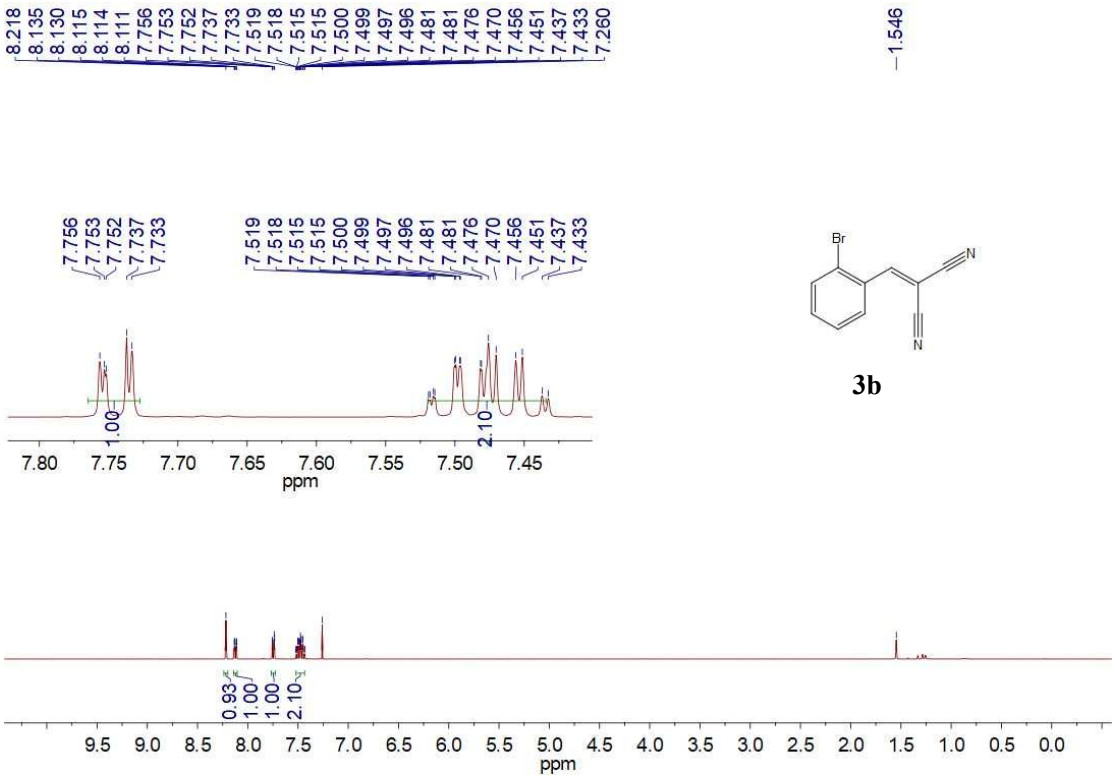

Figure S23. ^{1}H NMR spectra of **3b** (in $CDCl_3$).

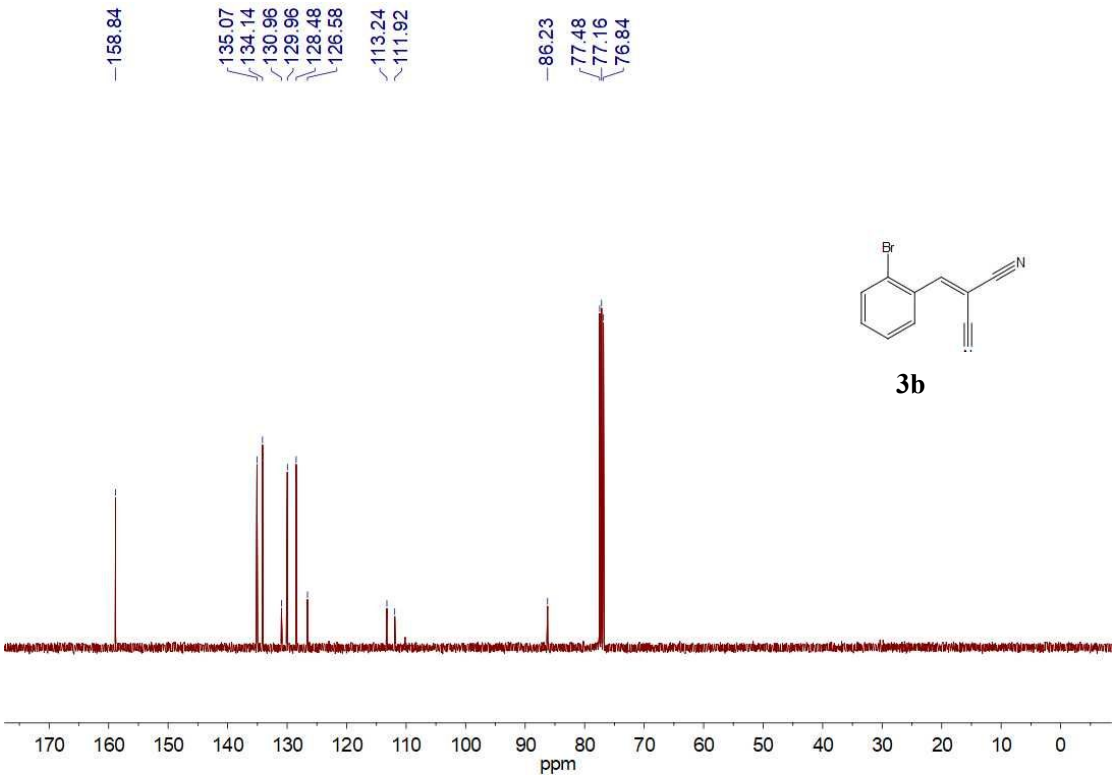

Figure S24. ^{13}C NMR spectrum of **3b** (in $CDCl_3$).

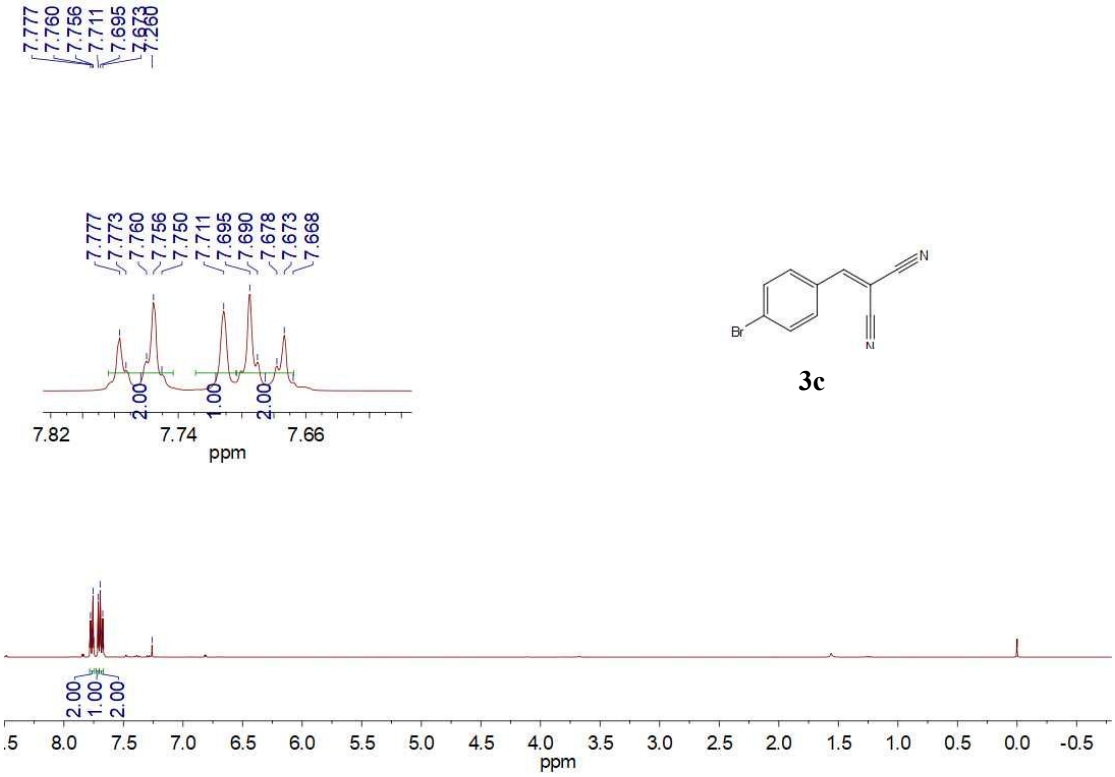

Figure S25. ^{1}H NMR spectra of **3c** (in $CDCl_3$)

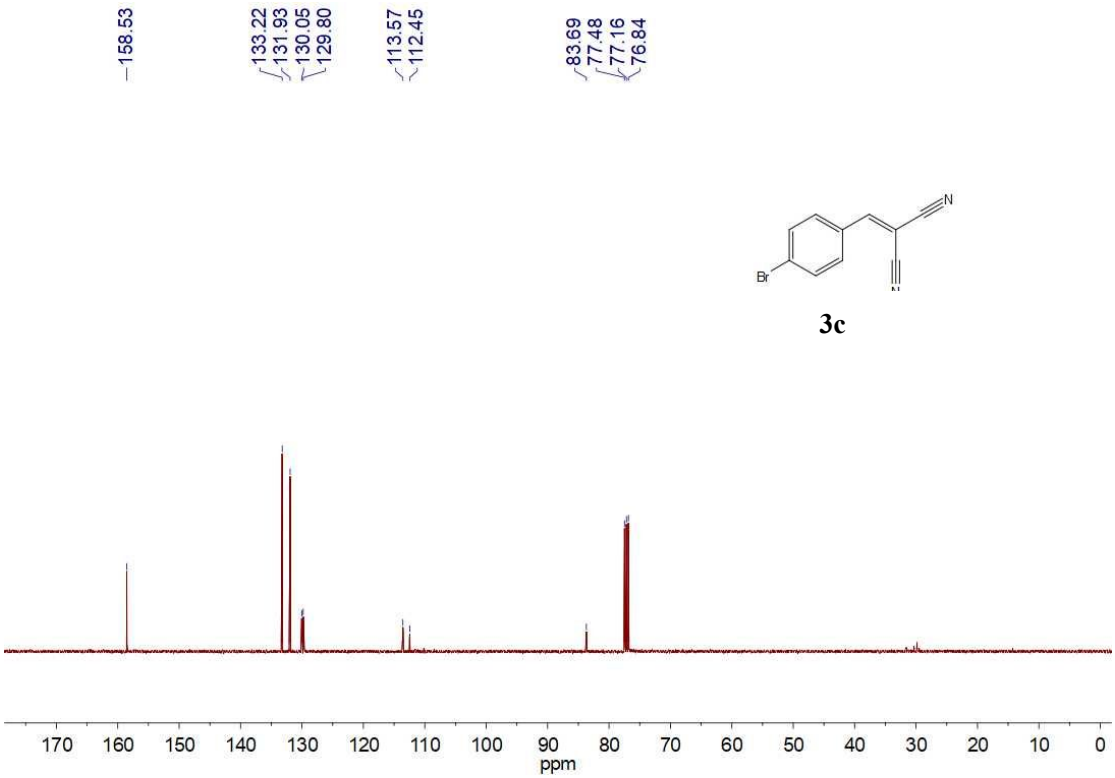

Figure S26. ^{13}C NMR spectrum of **3c** (in $CDCl_3$).

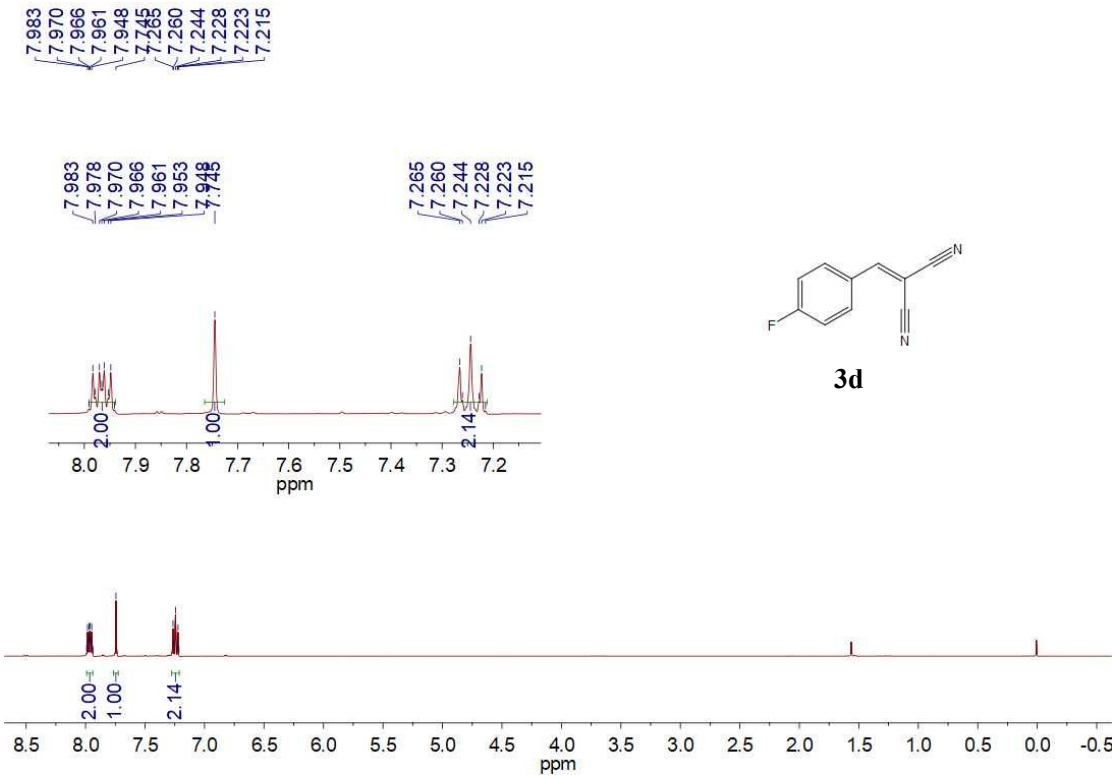

Figure S27. ^{1}H NMR spectra of **3d** (in $CDCl_3$).

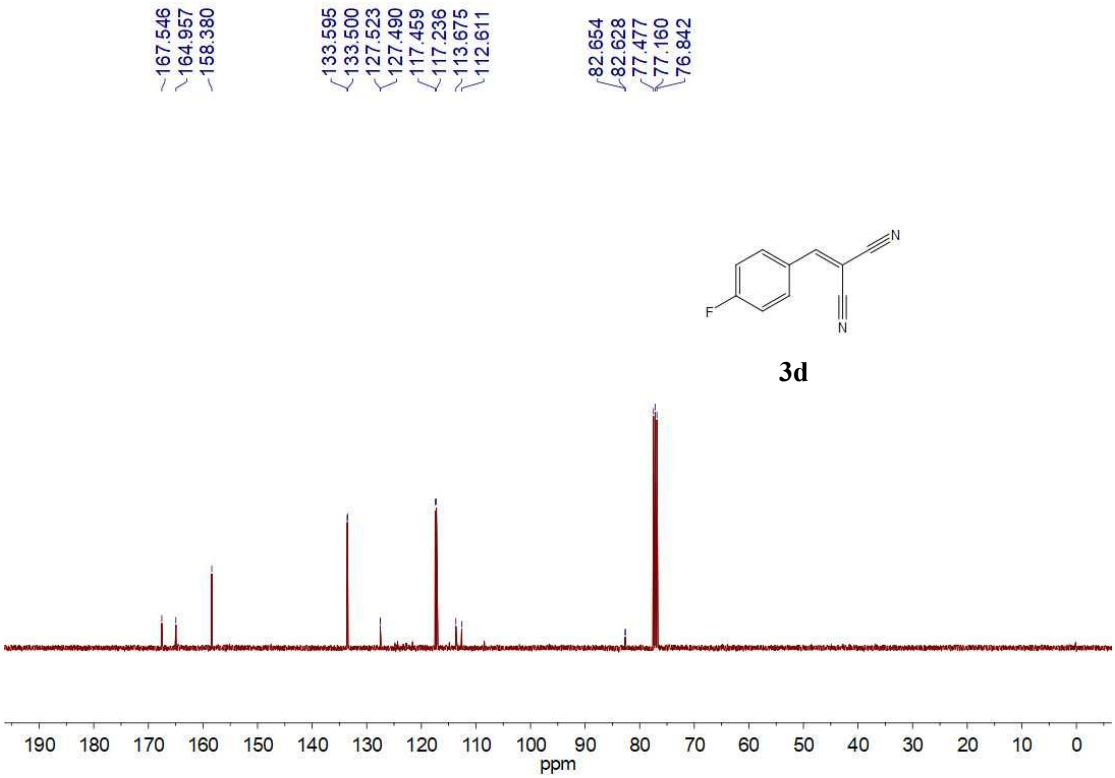

Figure S28. ^{13}C NMR spectrum of **3d** (in $CDCl_3$).

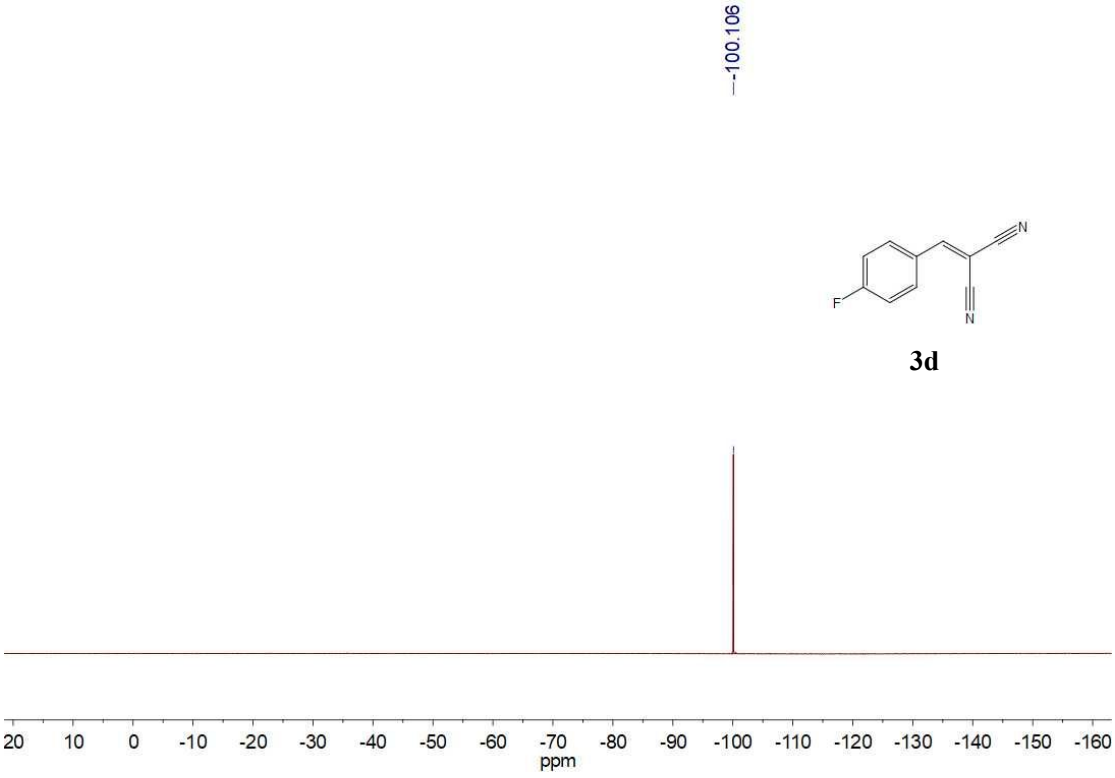

Figure S29. ^{19}F NMR spectrum of **3d** (in $CDCl_3$).

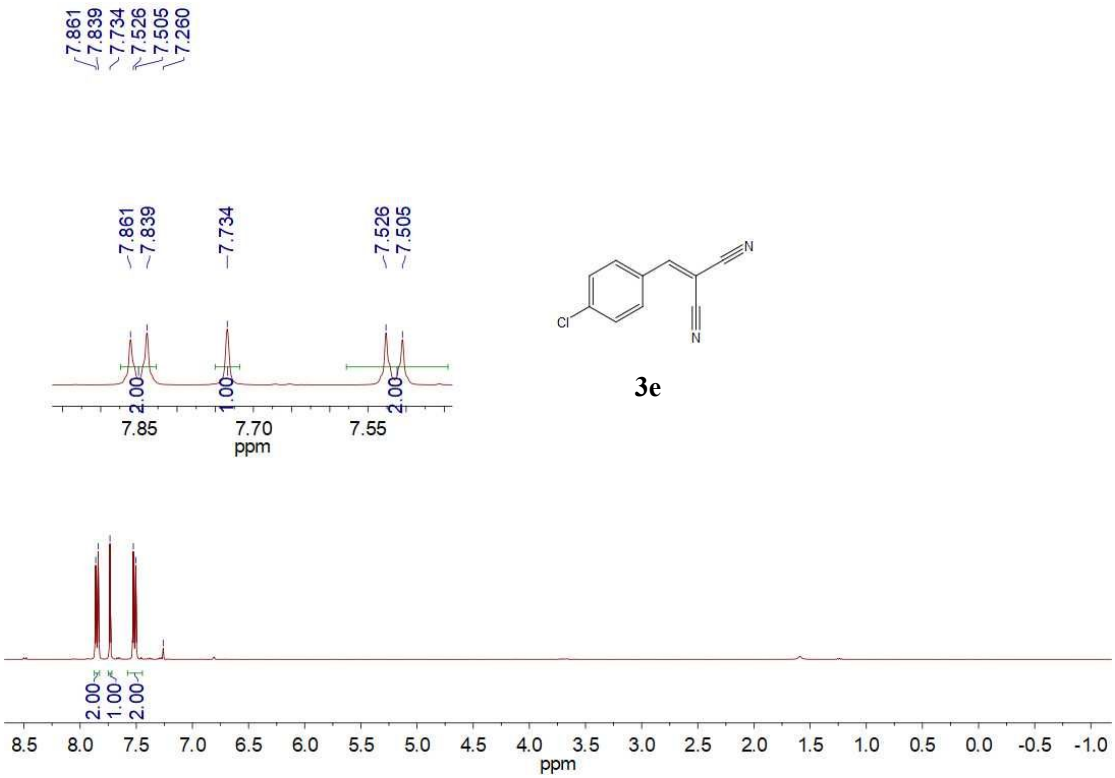

Figure S30. ^{1}H NMR spectra of **3e** (in $CDCl_3$).

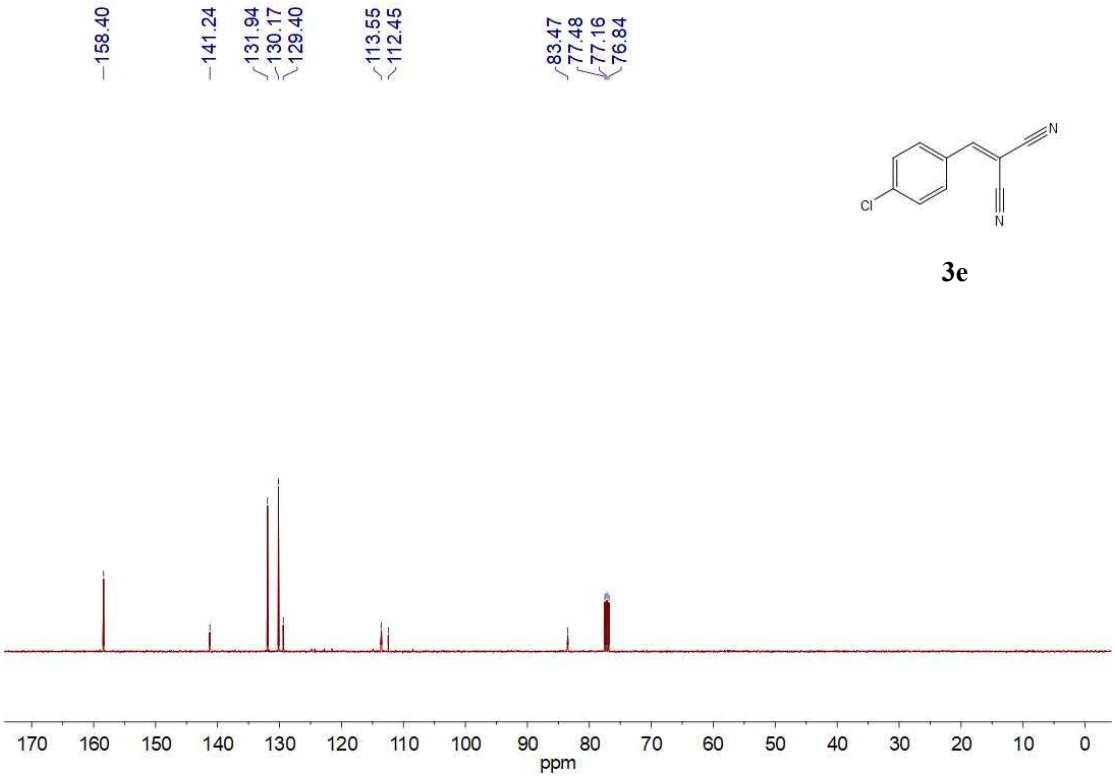

Figure S31. ^{13}C NMR spectrum of **3e** (in $CDCl_3$)

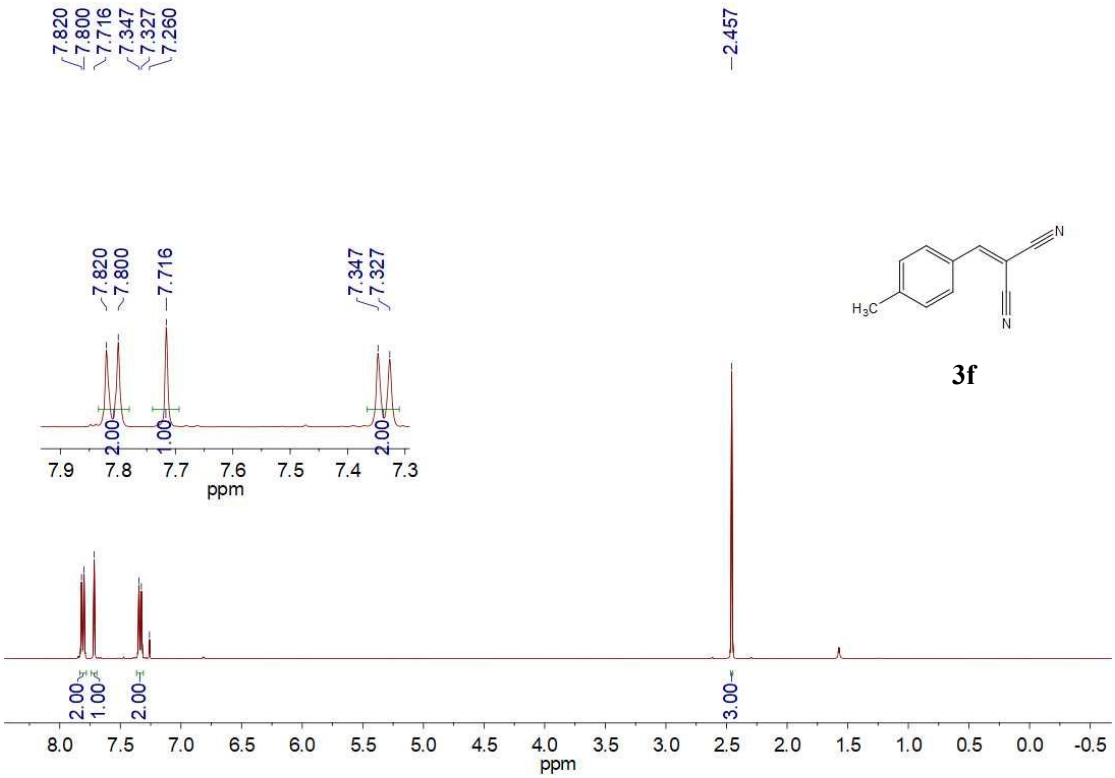

Figure S32. ^{1}H NMR spectra of **3f** (in $CDCl_3$).

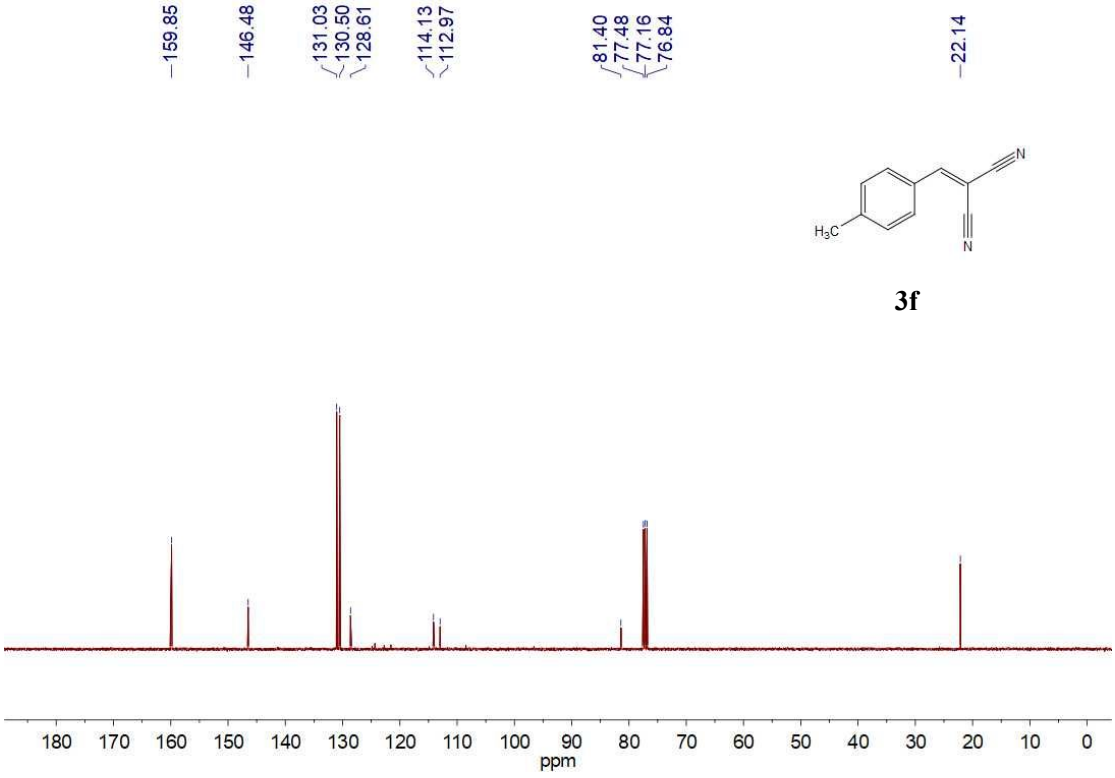

Figure S33. ^{13}C NMR spectrum of **3f** (in $CDCl_3$).

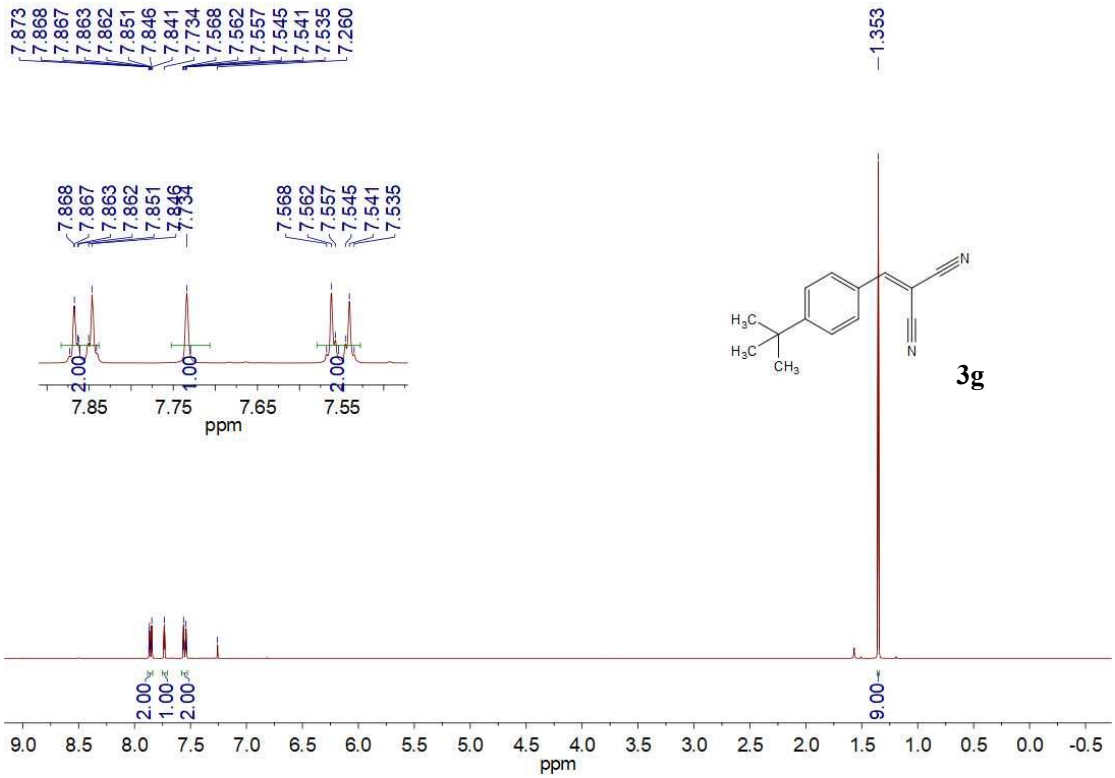

Figure S34. ^{1}H NMR spectra of **3g** (in $CDCl_3$).

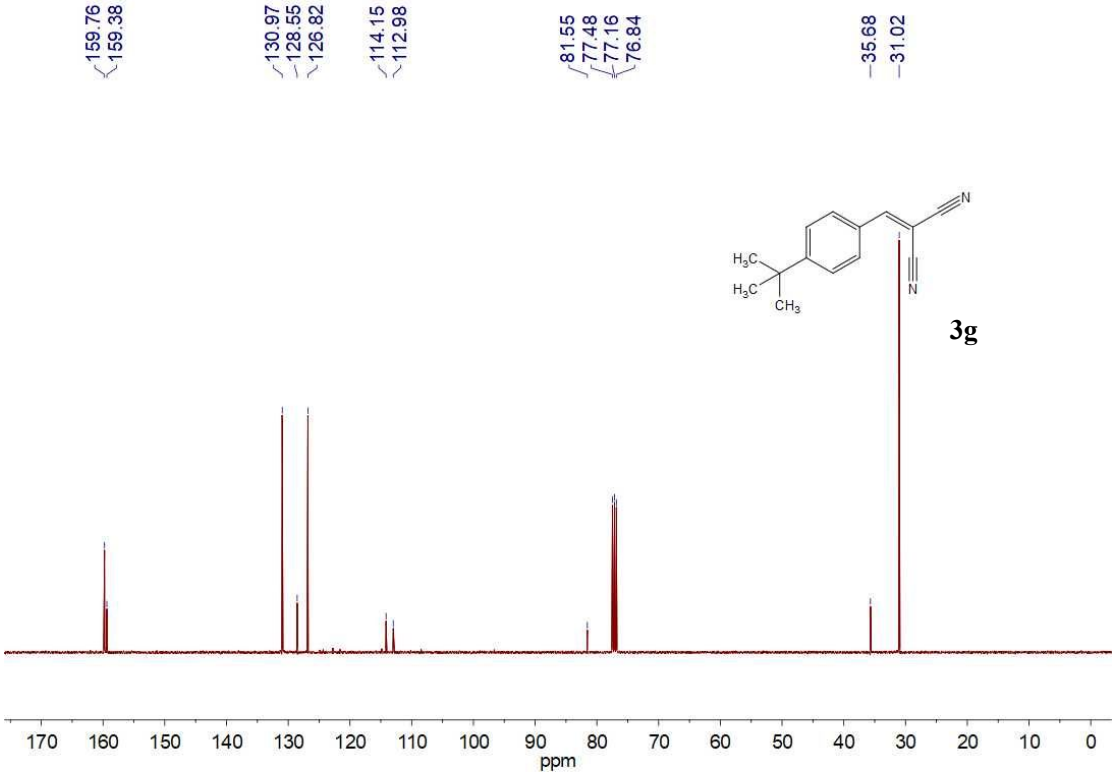

Figure S35. ^{13}C NMR spectrum of **3g** (in $CDCl_3$).

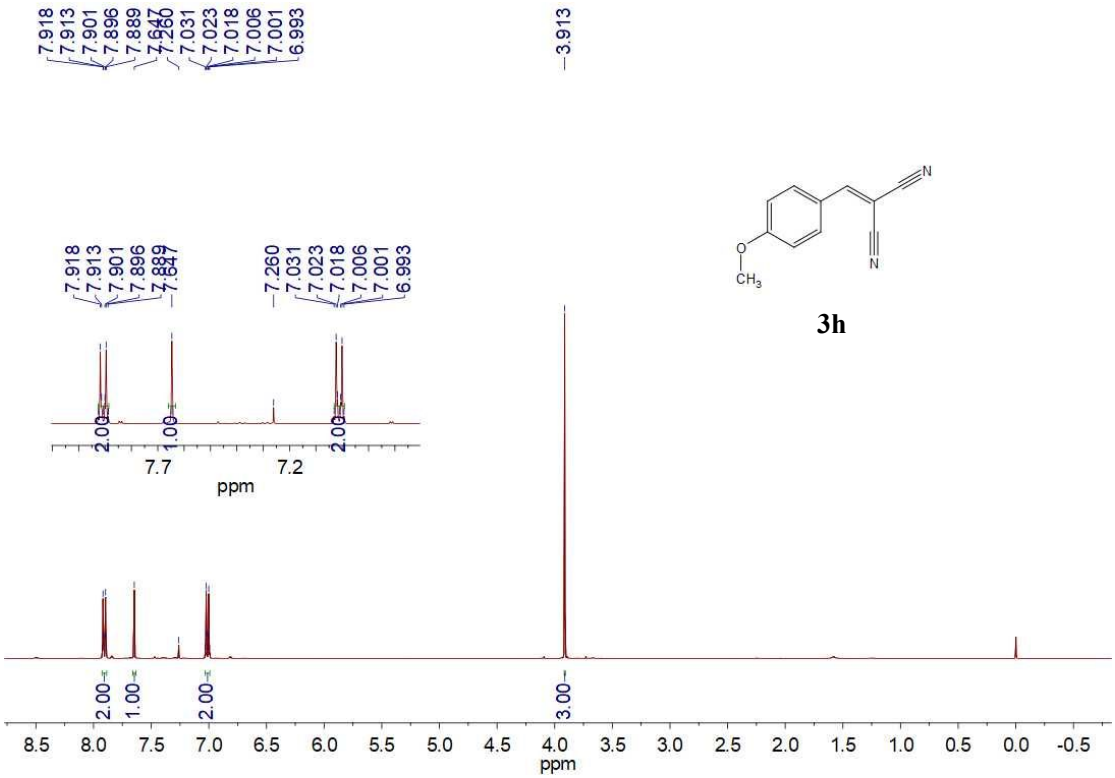

Figure S36. ^{1}H NMR spectra of **3h** (in $CDCl_3$).

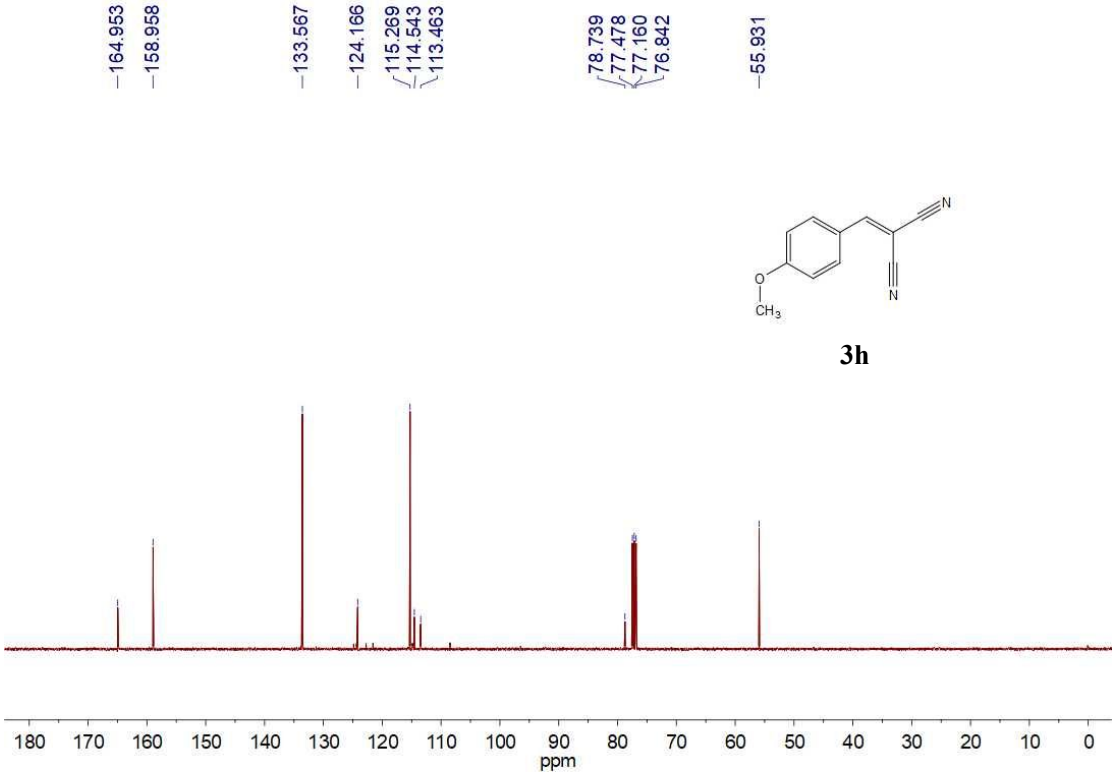

Figure S37. ^{13}C NMR spectrum of **3h** (in $CDCl_3$).

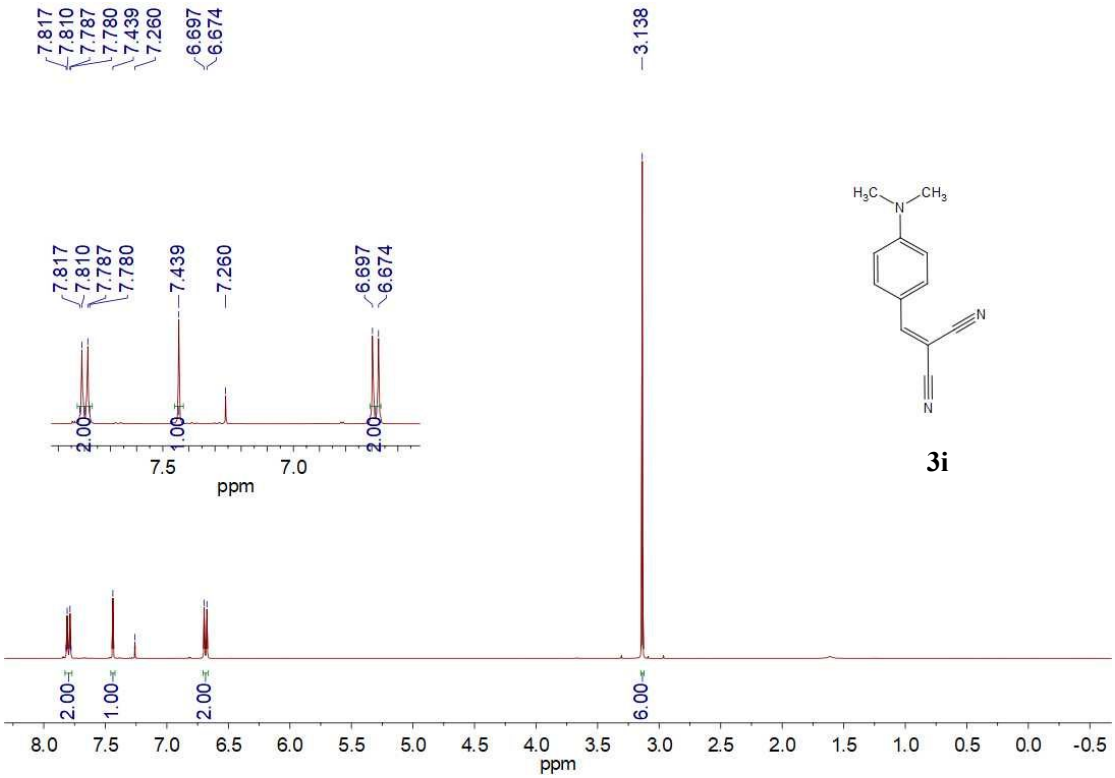

Figure S38. ^{1}H NMR spectra of **3i** (in $CDCl_3$).

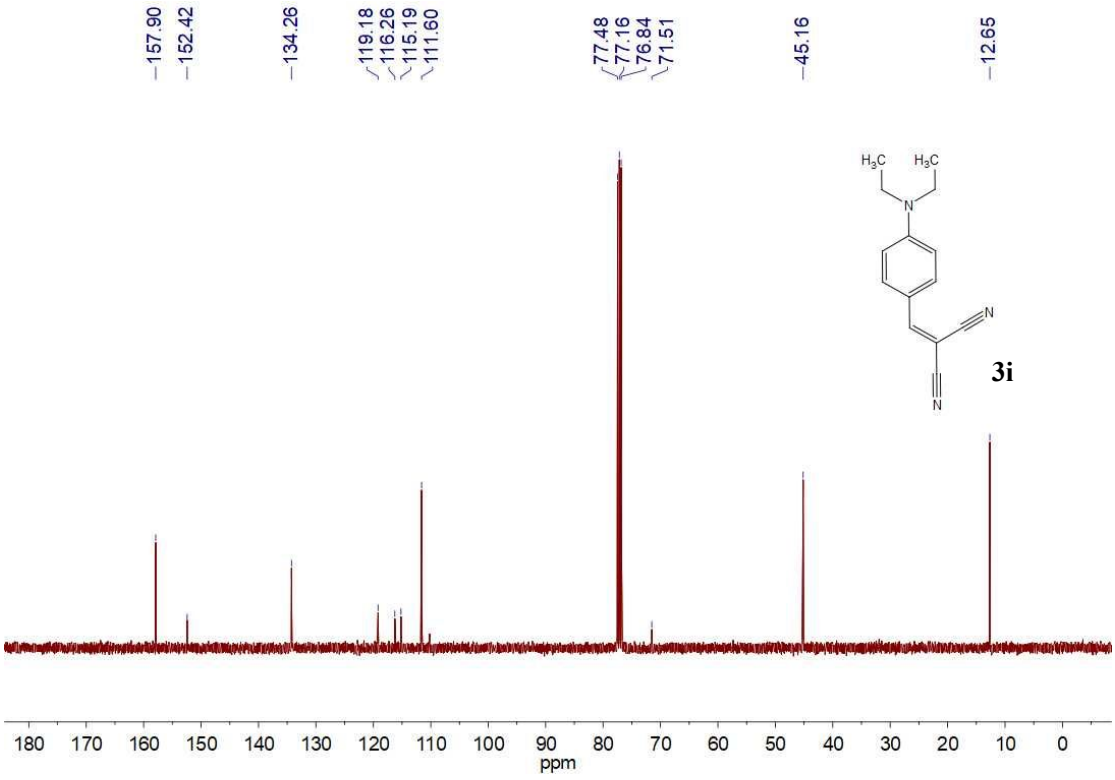

Figure S39. ^{13}C NMR spectrum of **3i** (in $CDCl_3$).

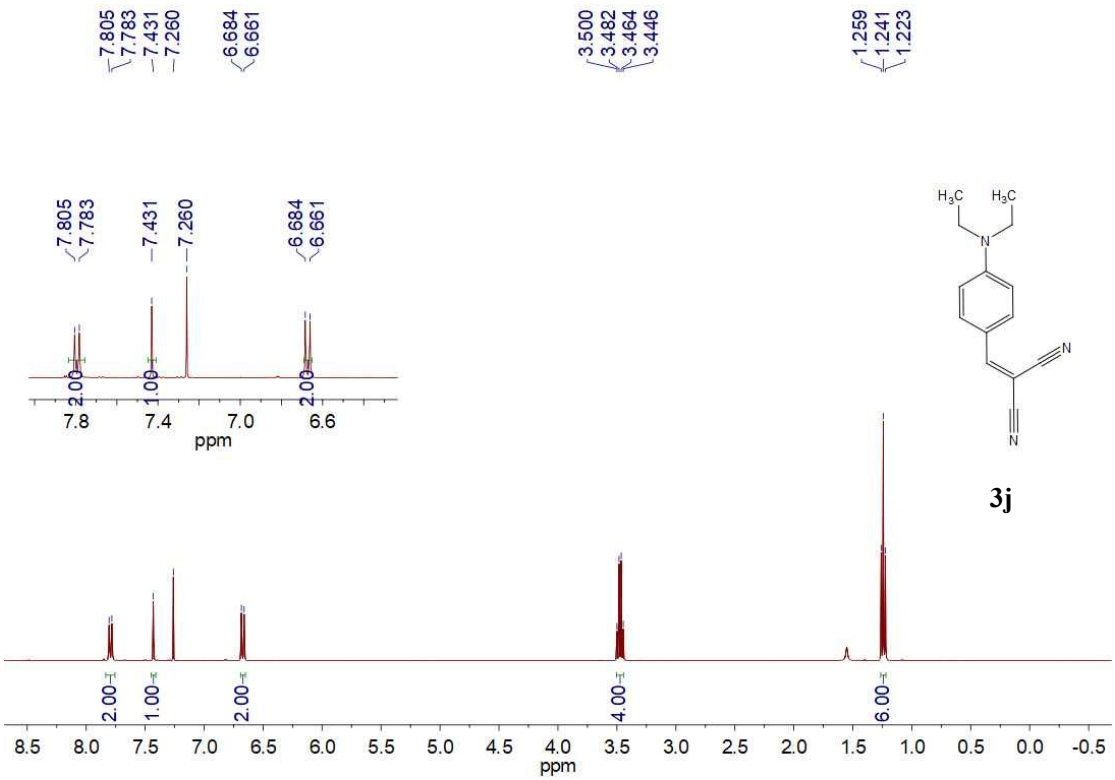

Figure S40. ^{1}H NMR spectra of **3j** (in $CDCl_3$).

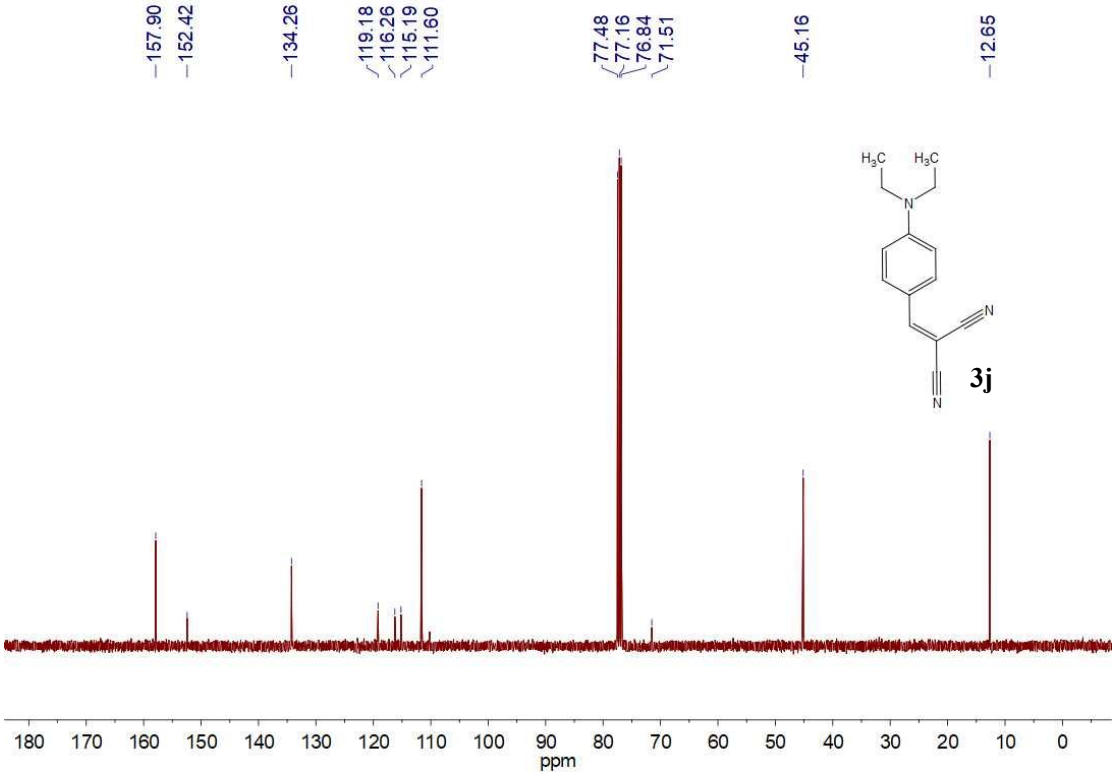

Figure S41. ^{13}C NMR spectrum of **3j** (in $CDCl_3$).

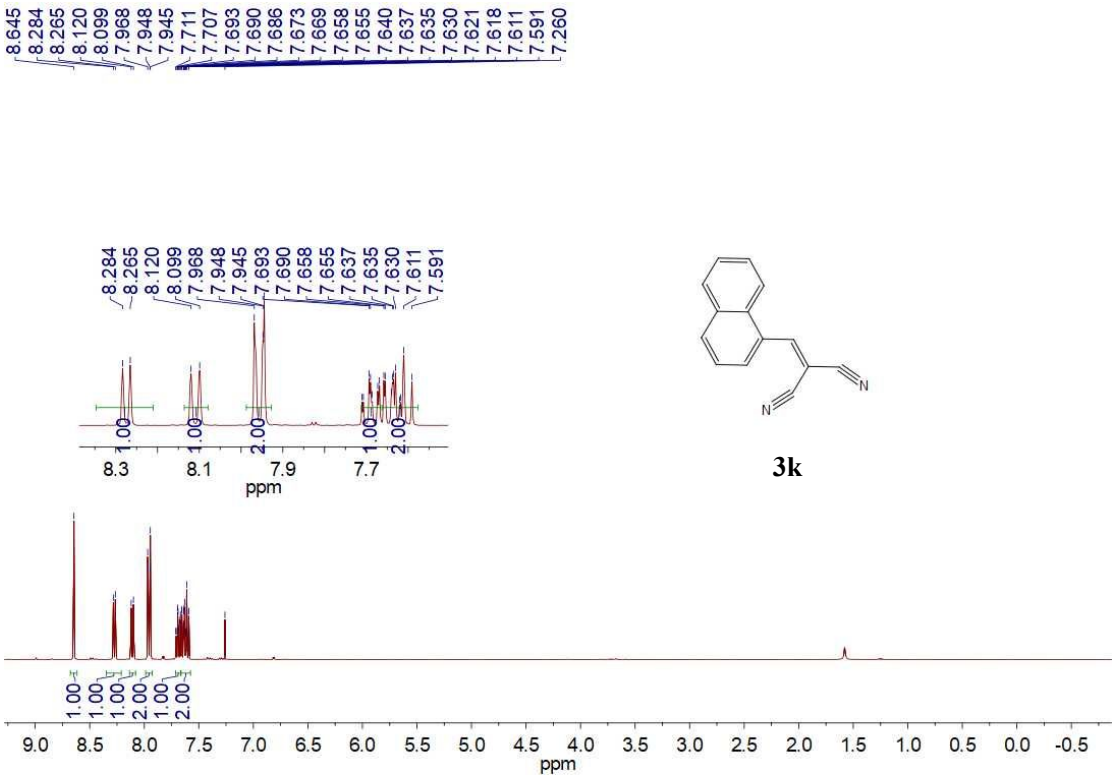

Figure S42. ^{1}H NMR spectra of **3k** (in $CDCl_3$).

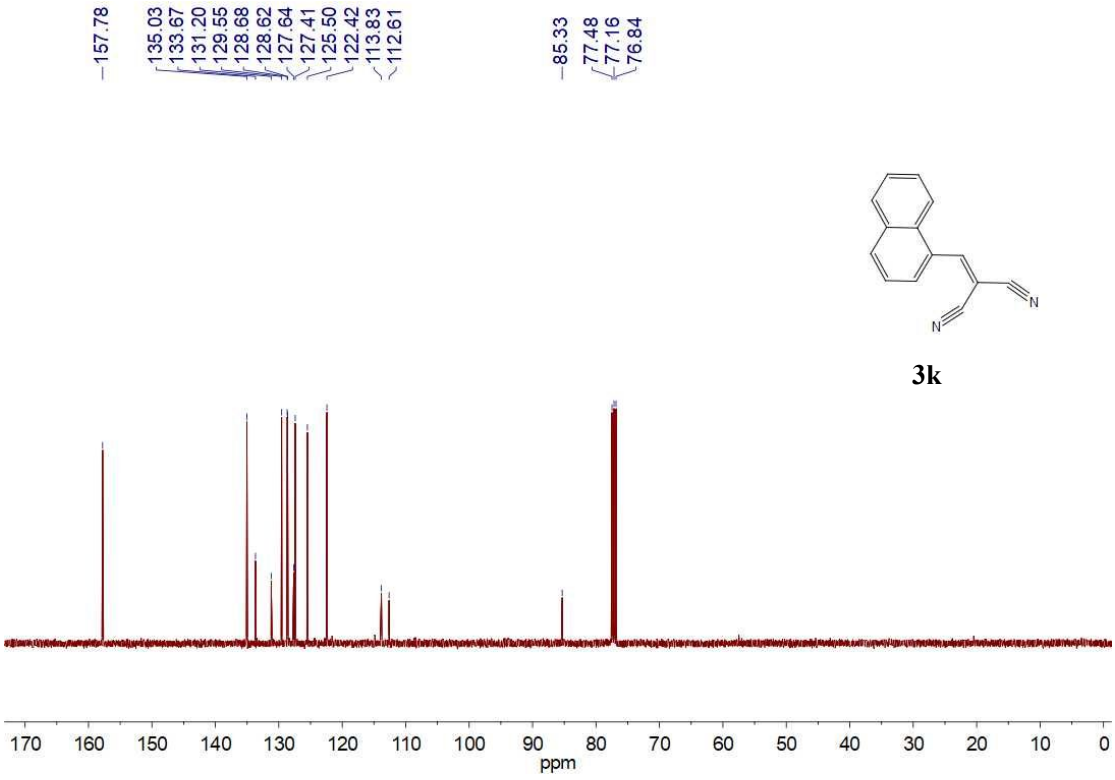

Figure S43. ^{13}C NMR spectrum of **3k** (in $CDCl_3$).

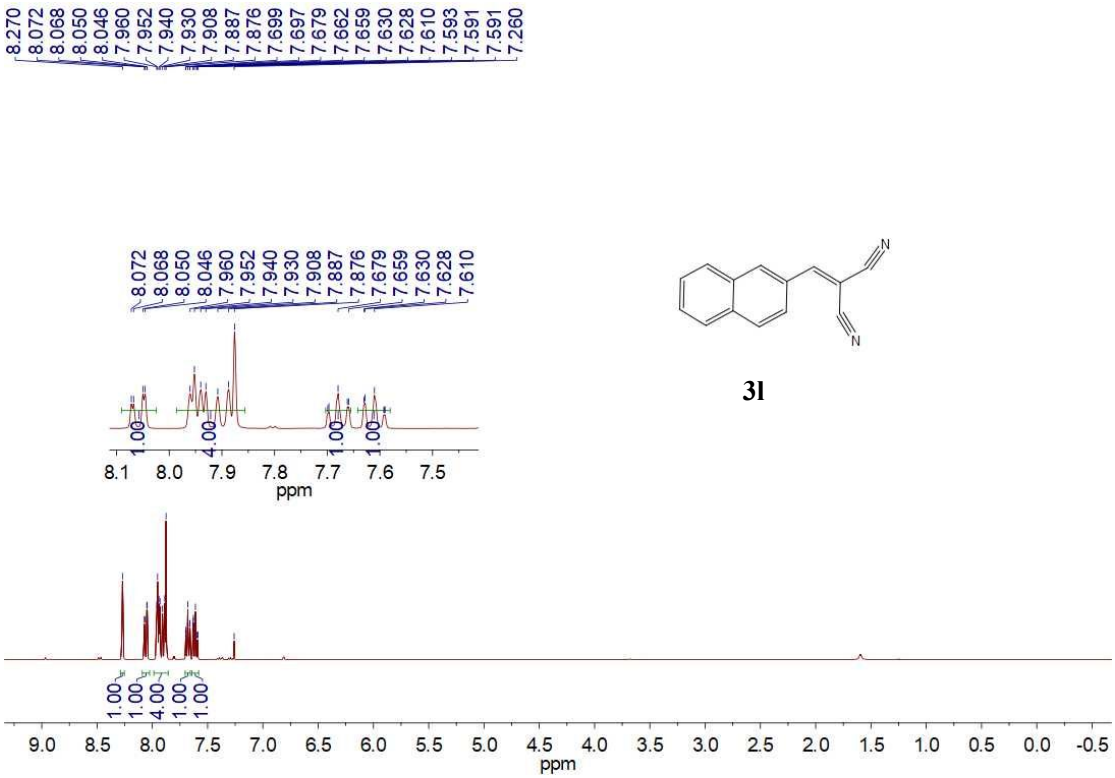

Figure S44. ^{1}H NMR spectra of **3l** (in $CDCl_3$).

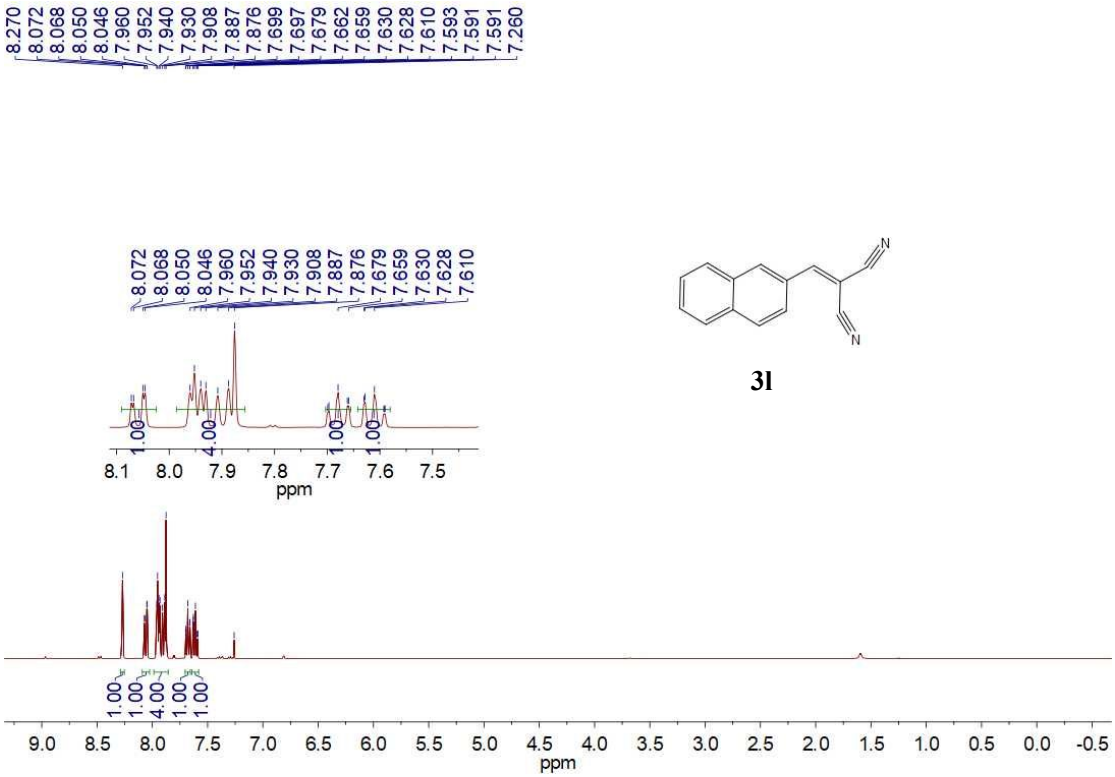

Figure S45. ^{13}C NMR spectrum of **3l** (in $CDCl_3$).

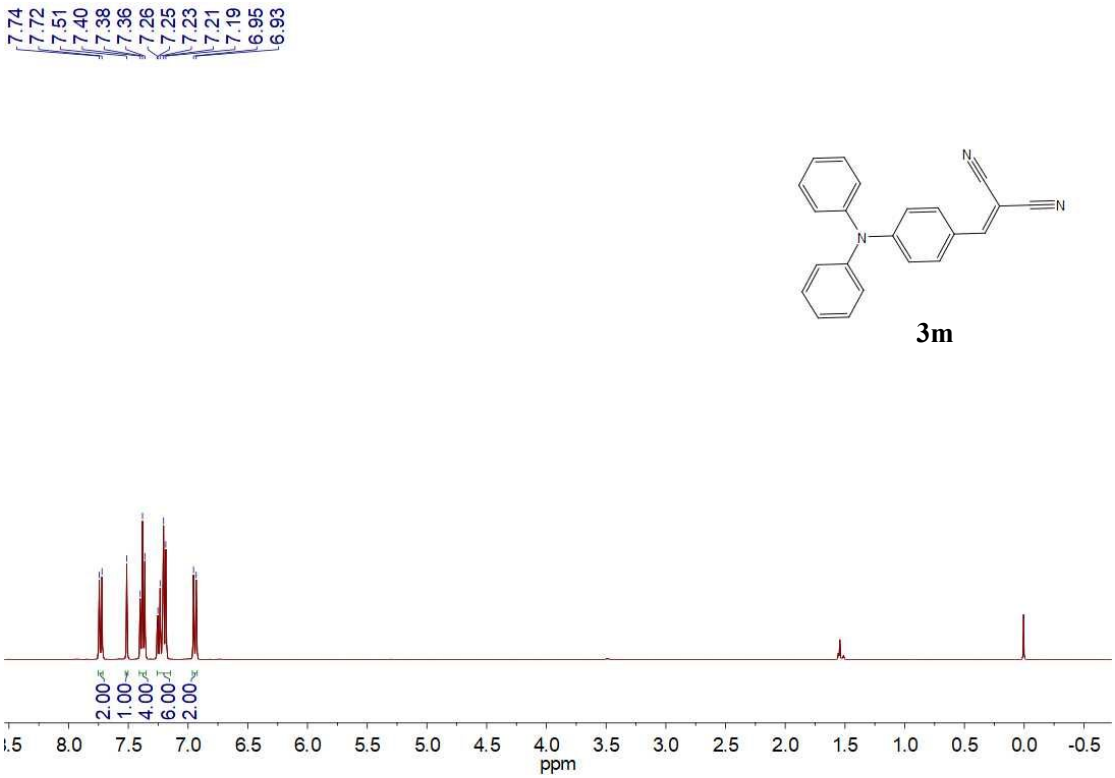

Figure S46. ^{1}H NMR spectrum of **3m** (in $CDCl_3$).

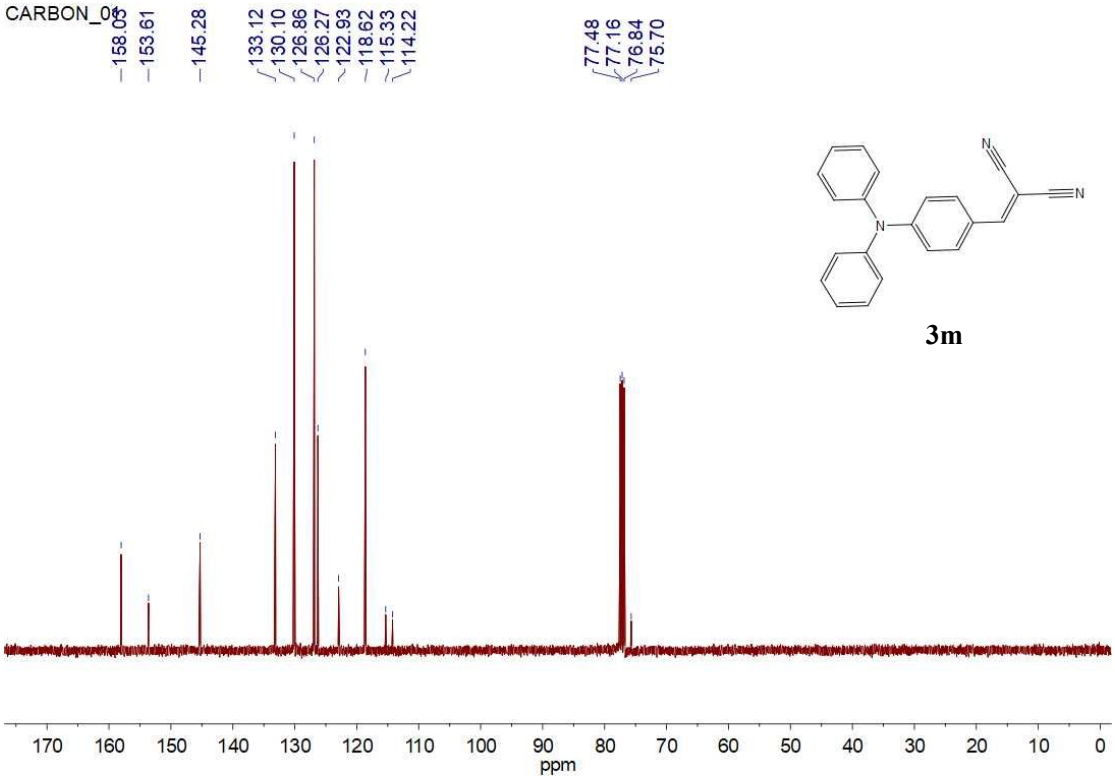

Figure S47. ^{13}C NMR spectrum of **3m** (in $CDCl_3$).

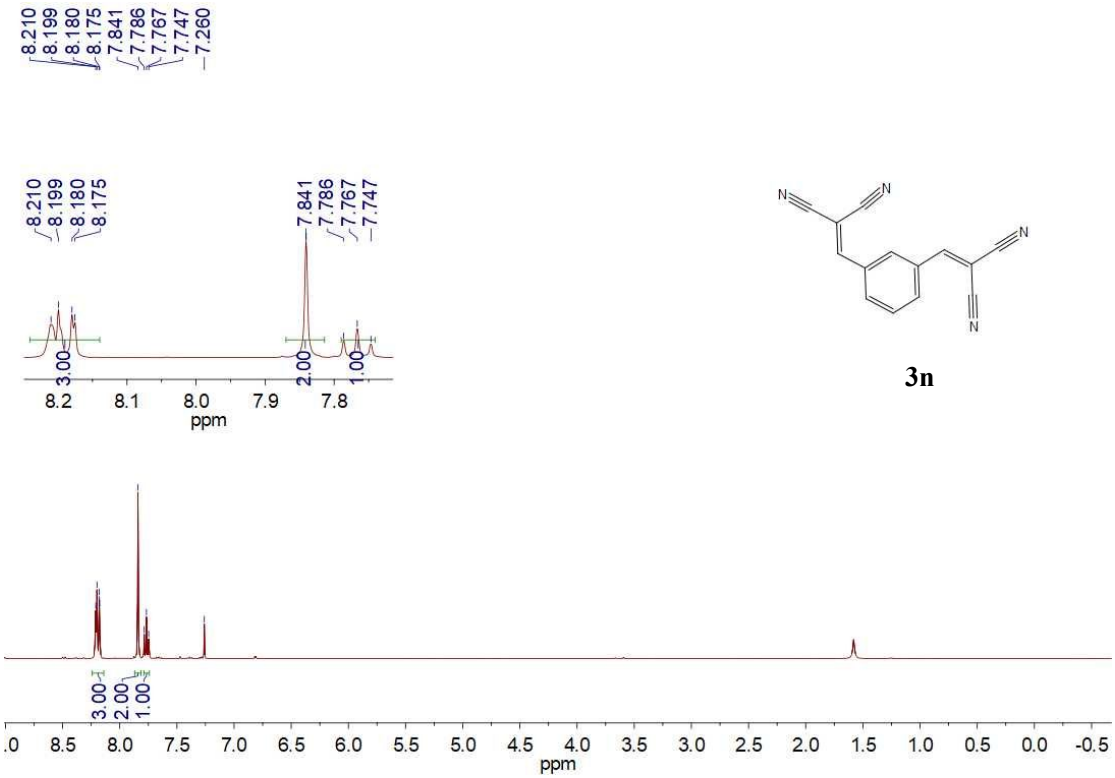

Figure S48. ^{1}H NMR spectra of **3n** (in $CDCl_3$).

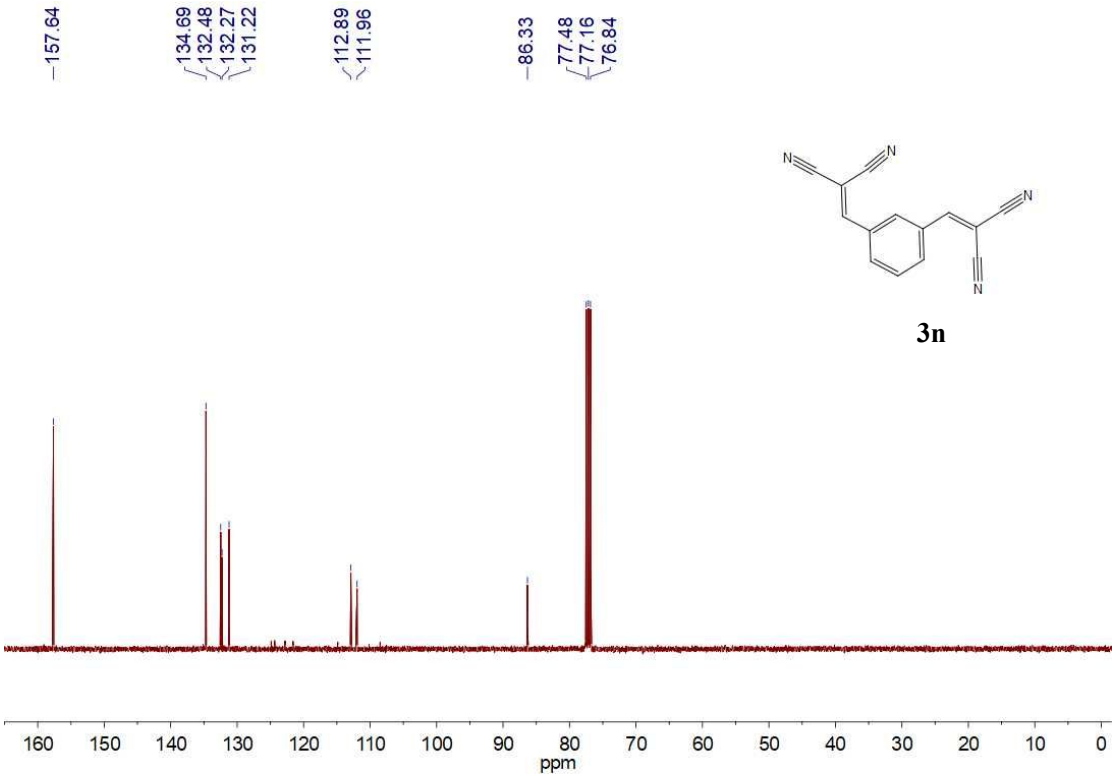

Figure S49. ^{13}C NMR spectrum of **3n** (in $CDCl_3$).

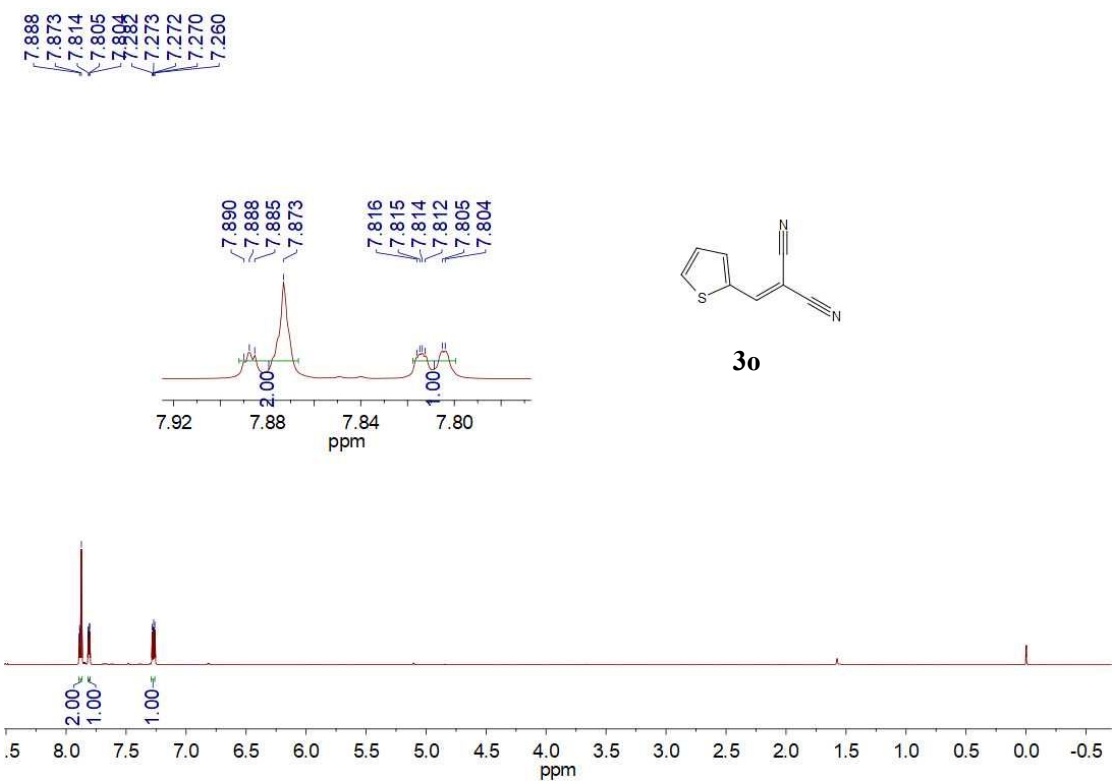

Figure S50. ^{1}H NMR spectra of **3o** (in $CDCl_3$).

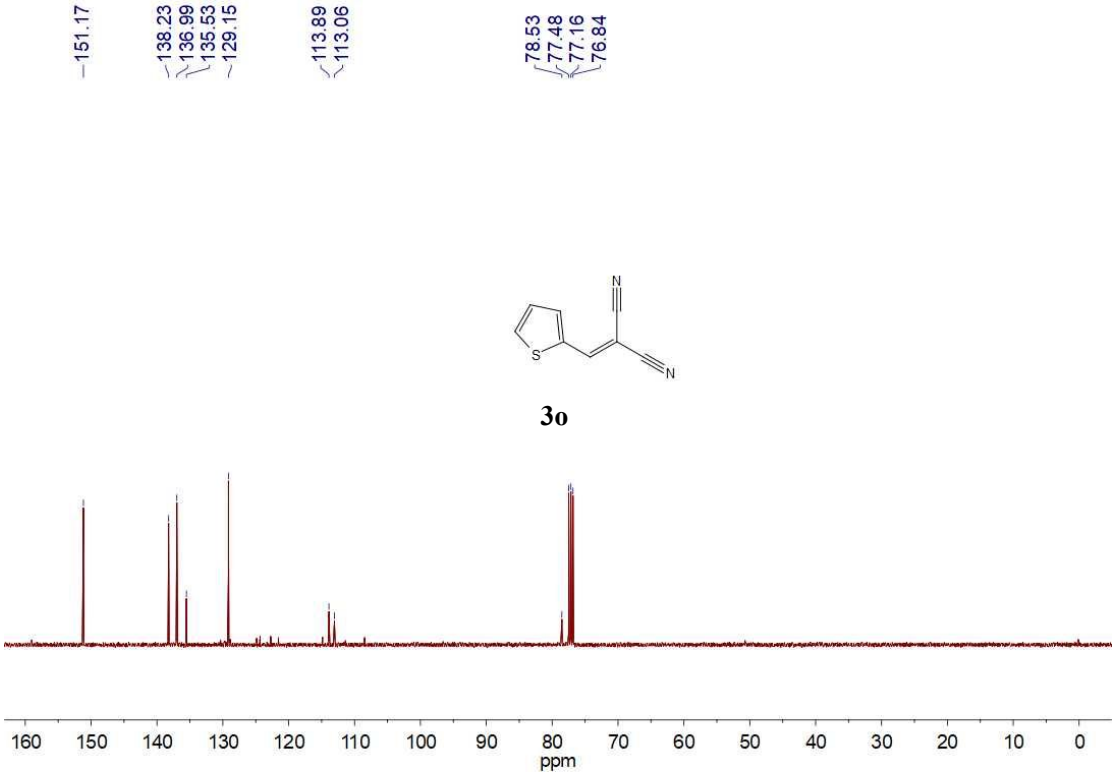

Figure S51. ^{13}C NMR spectrum of **3o** (in $CDCl_3$).

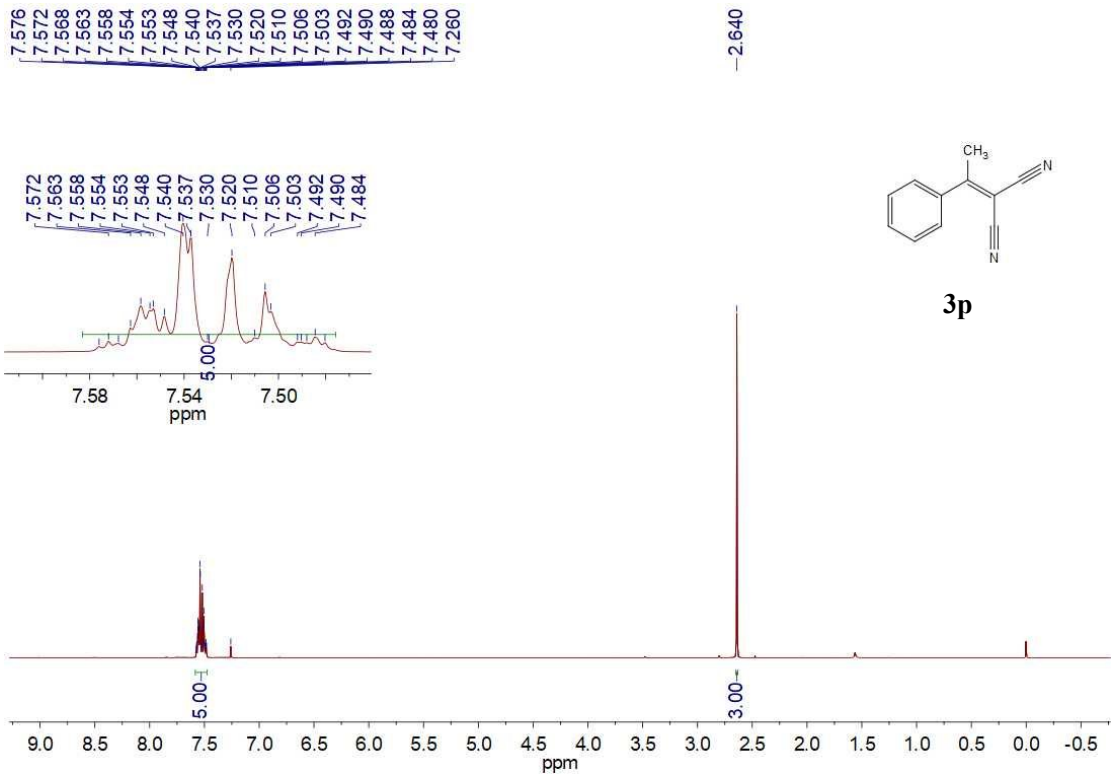

Figure S52. ^{1}H NMR spectra of **3p** (in $CDCl_3$).

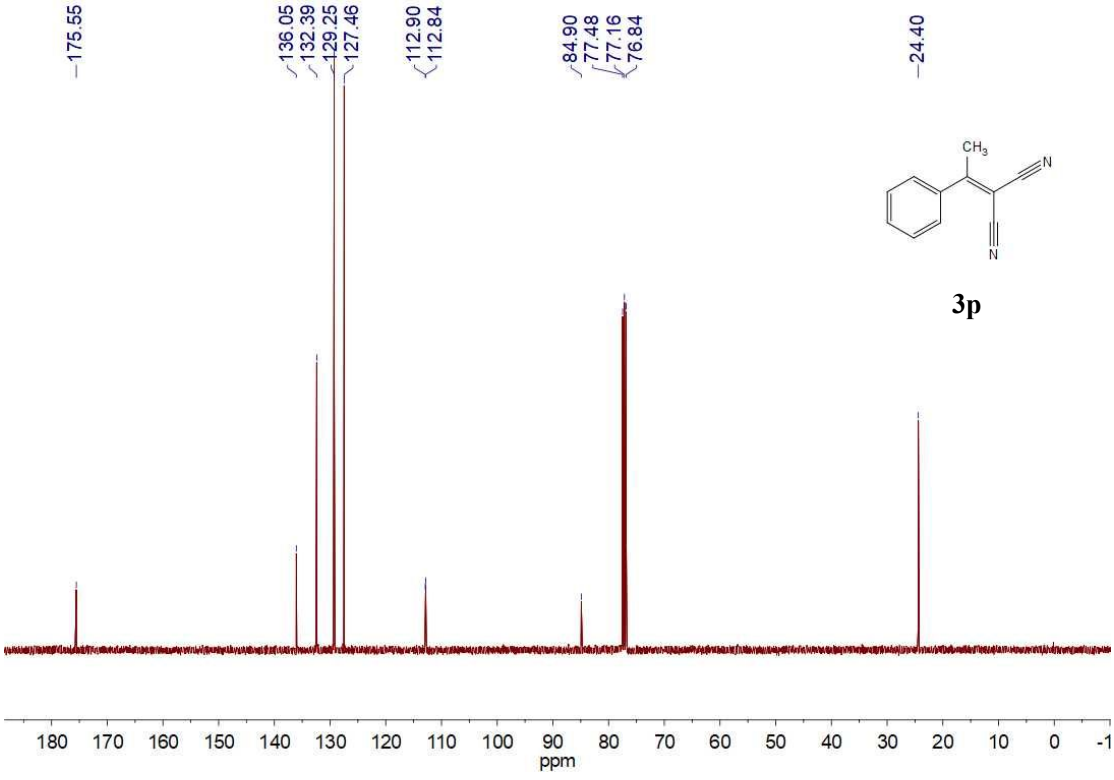

Figure S53. ^{13}C NMR spectrum of **3p** (in $CDCl_3$).

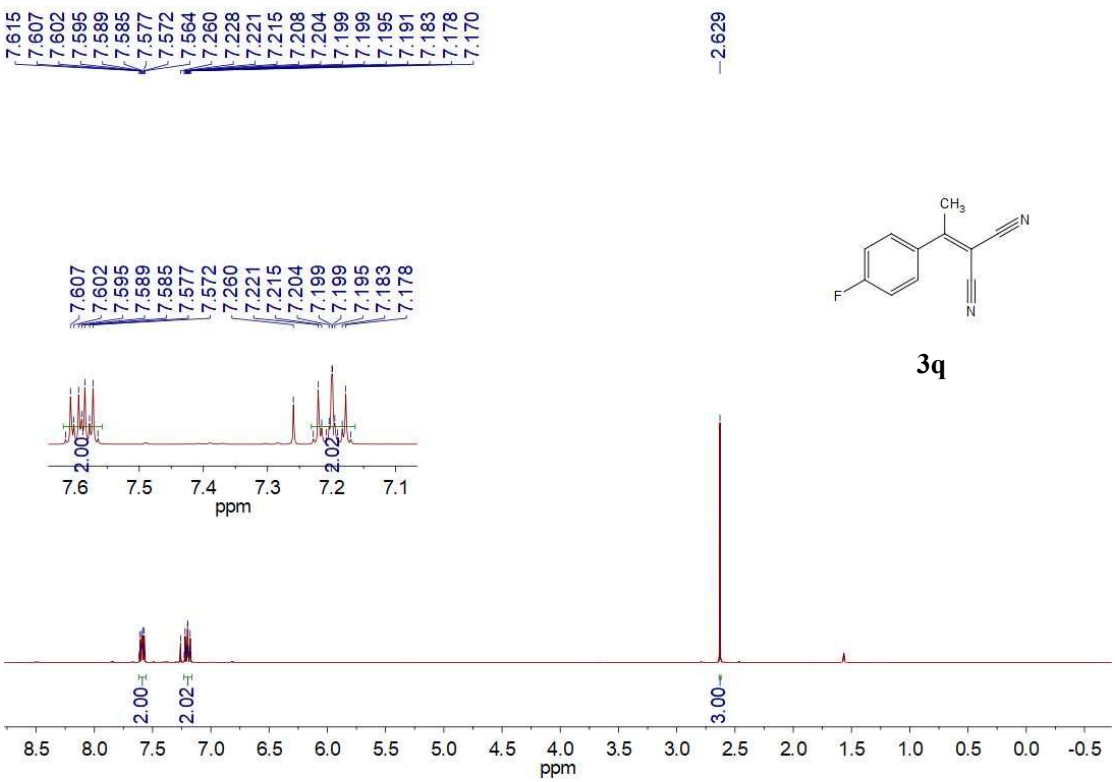

Figure S54. ^{1}H NMR spectra of **3q** (in $CDCl_3$).

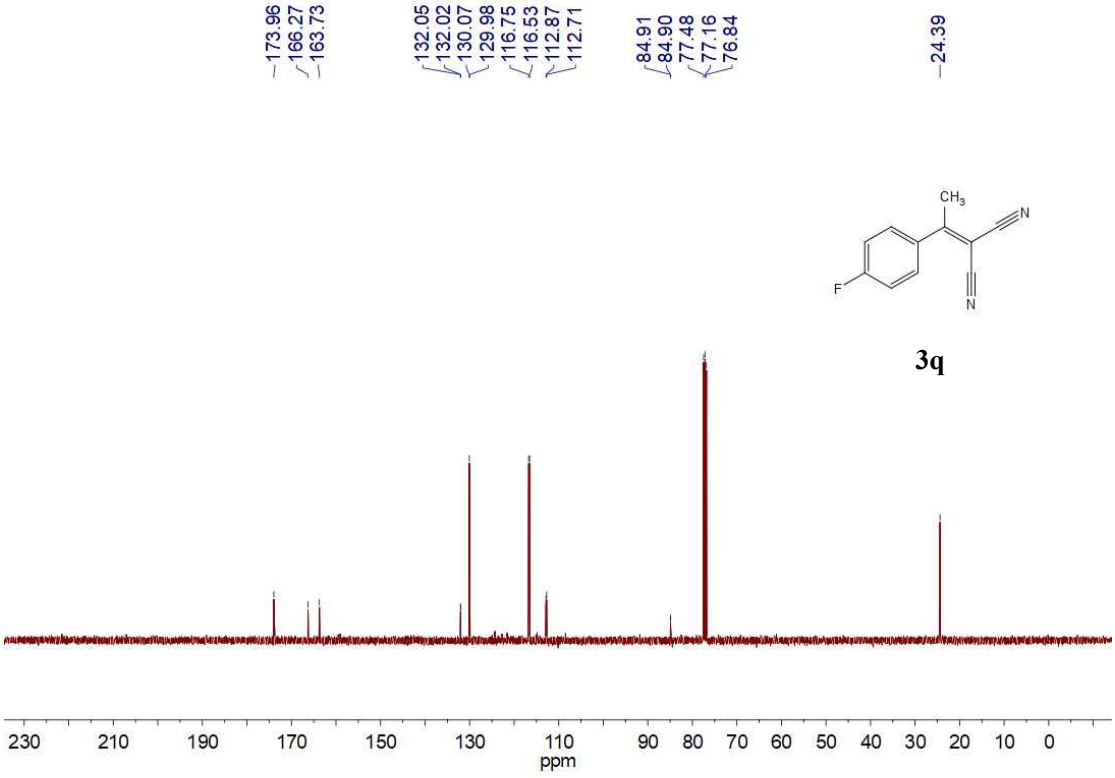

Figure S55. ^{13}C NMR spectrum of **3q** (in $CDCl_3$).

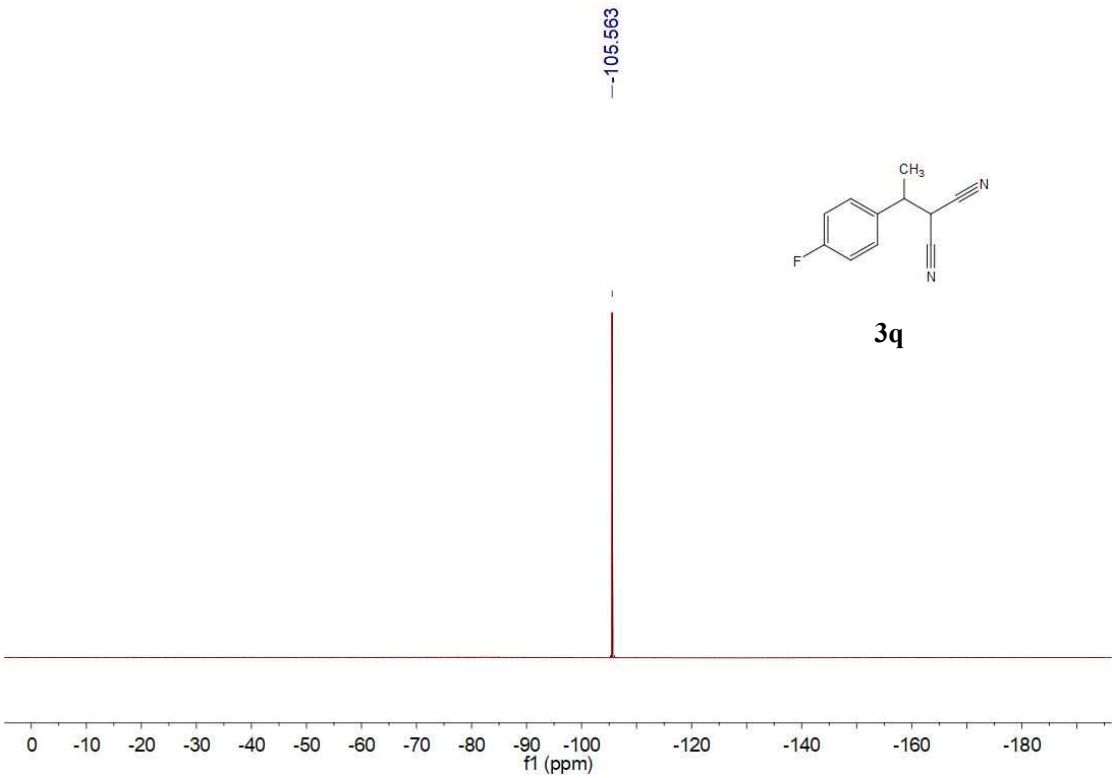

Figure S56. ^{19}F NMR spectrum of **3q** (in $CDCl_3$).

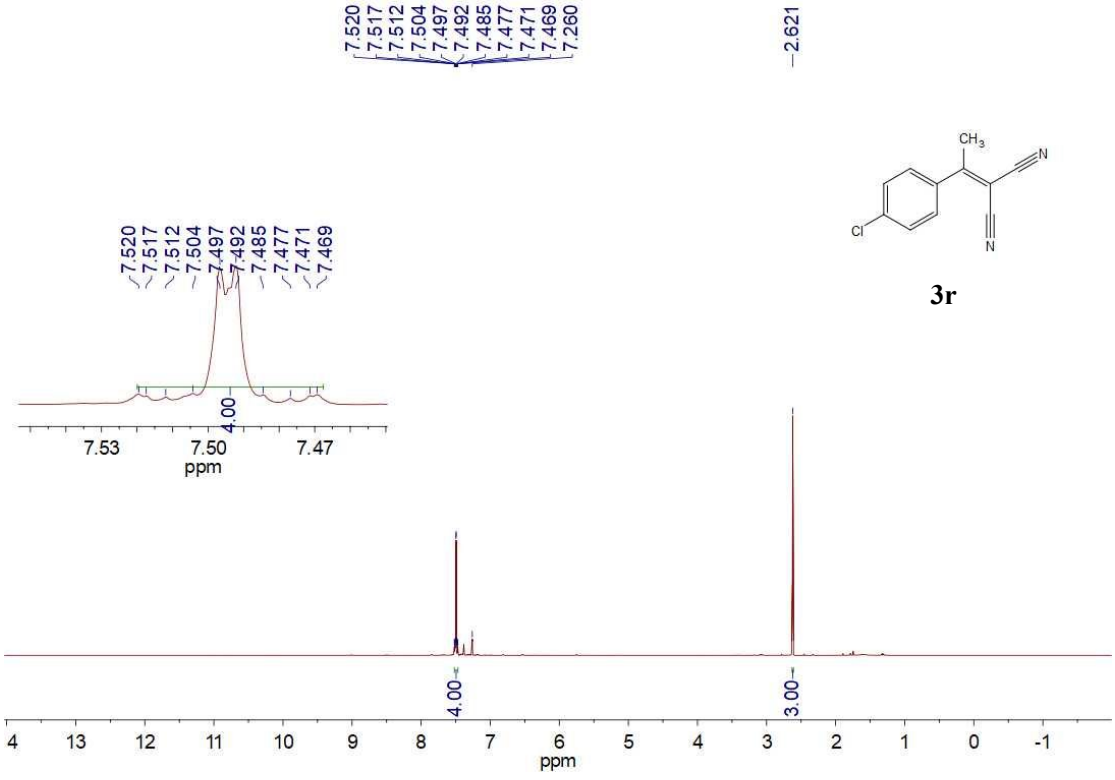

Figure S57. ^{1}H NMR spectra of **3r** (in $CDCl_3$).

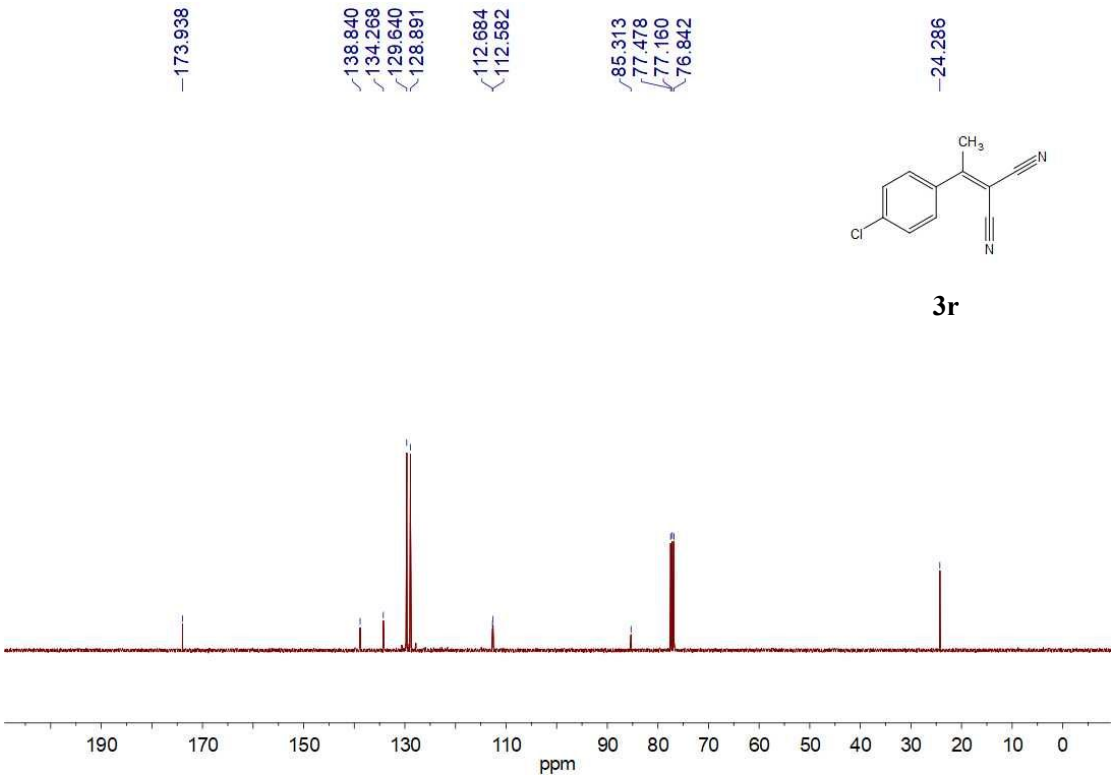

Figure S58. ^{13}C NMR spectrum of **3r** (in $CDCl_3$).

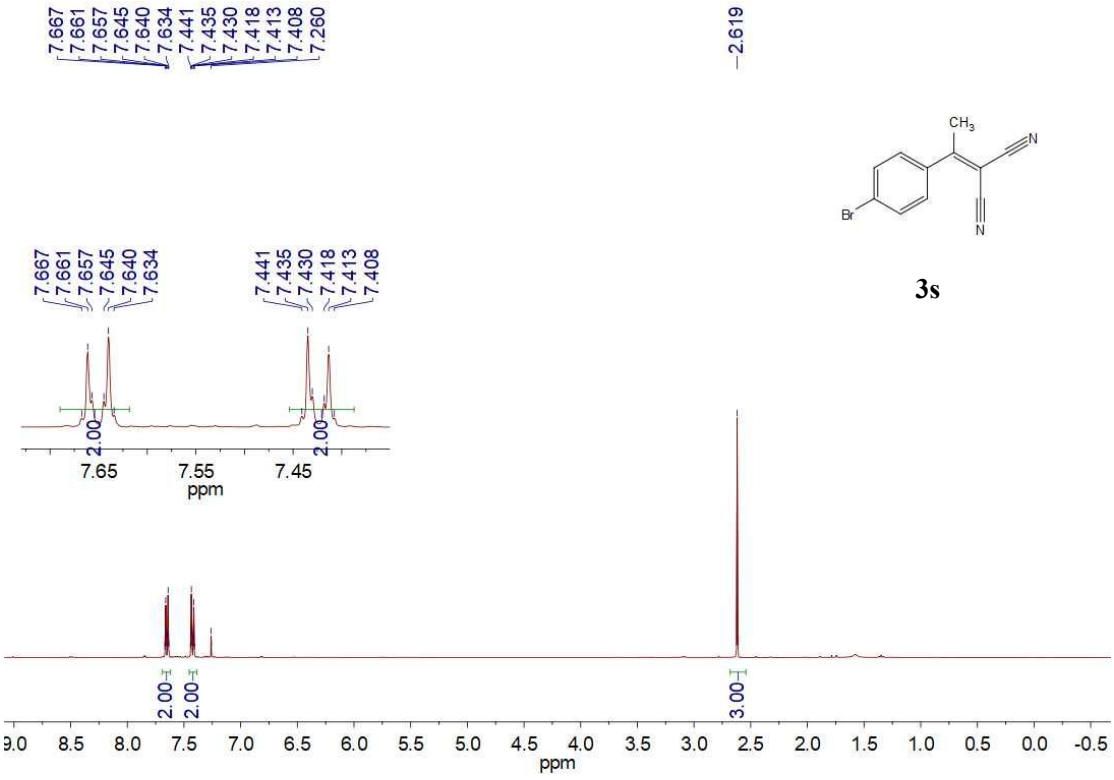

Figure S59. ^{1}H NMR spectra of **3s** (in $CDCl_3$).

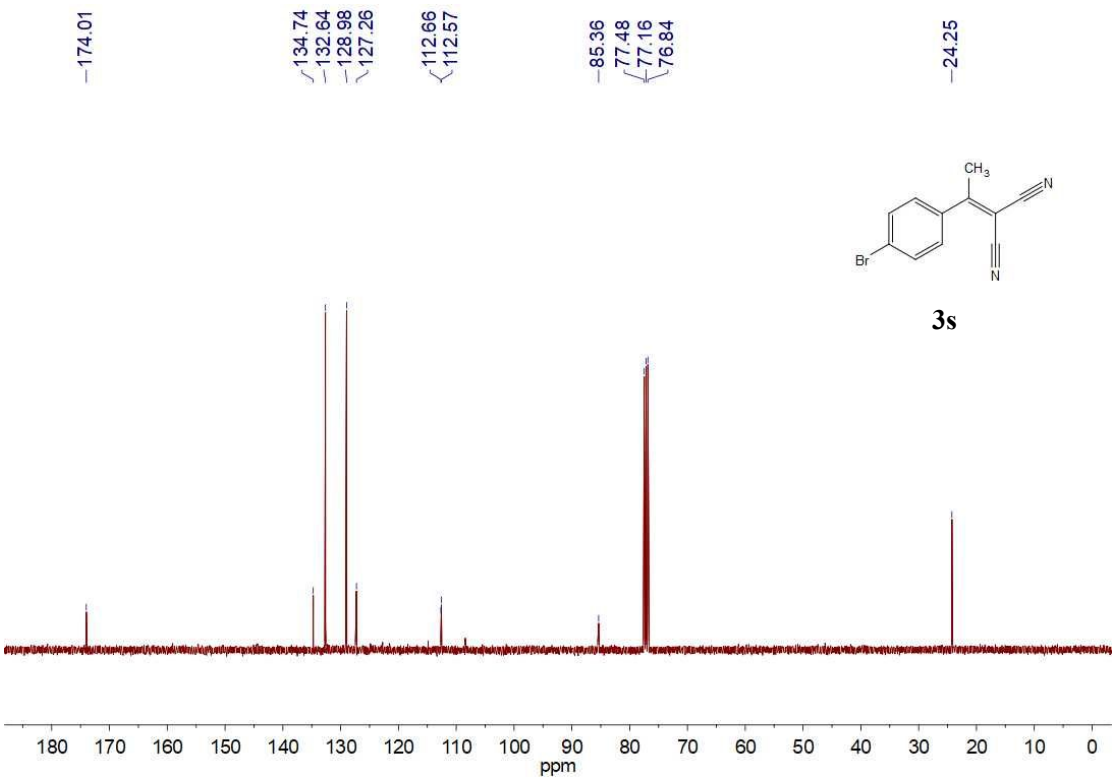

Figure S60. ^{13}C NMR spectrum of **3s** (in $CDCl_3$).

Section E. References

[S1]. Song, Q.; Goia, S.; Yang, J.; Hall, S. C. L.; Staniforth, M.; Stavros, V. G.; Perrier, S. *J. Am. Chem. Soc*. **2021**, *143*, 382-389.

[S2]. Li, Y. W.; Dong, Y. H.; Cheng, L.; Qin, C. Y.; Nian, H.; Zhang, H. Y.; Yu, Y.; Cao, L. P. *J. Am. Chem. Soc*. **2019**, *141*, 8412-8415.

[S3]. Yuan, Y. X.; Jia, J. H.; Song, Y. P.; Ye, F.Y.; Zheng, Y.-S.; Zang, S. Q. *J. Am. Chem.Soc*. **2022**, *144*, 5389-539